SUPPORTING INFORMATION

Selectivity of *N(2)*-substituted oxotriazinoindole aldose reductase inhibitors is determined by the interaction pattern with Pro301-Arg312 loop of aldehyde reductase

Lucia Kováčiková [a,b*], Sunil Gaikwad [b], Kristína Almášiová [b], Ambroz Almássy [b], Gabriela Addová [b], Magdaléna Májeková [a], Gilles Hanquet [c], Vladimir Dobričić [d], Andrej Boháč [b,e#] and Milan Štefek [a#]

[a] *Institute of Experimental Pharmacology and Toxicology, CEM, SAS, Dúbravská cesta 9, 841 04 Bratislava, Slovakia*
[b] *Department of Organic Chemistry, Faculty of Natural Sciences, Comenius University in Bratislava, Ilkovičova 6, 842 15 Bratislava, Slovakia*
[c] *Université de Strasbourg, Université de Haute-Alsace, CNRS, UMR 7042-LIMA, ECPM, 25 rue Becquerel, 67087 Strasbourg, France*
[d] *Department of Pharmaceutical Chemistry, University of Belgrade – Faculty of Pharmacy, Vojvode Stepe 450, 112 21 Belgrade, Serbia*
[e] *Biomagi, Ltd., Mamateyova 26, 851 04 Bratislava, Slovakia*
[*] E-mail: lucia.kovacikova@savba.sk; # group leaders of medicinal chemistry and pharmacology

ABSTRACT: Novel oxotriazinoindoles (**OTI**s) were recently reported as highly efficient and selective aldose reductase inhibitors. Here, a series of novel *N(2)*-substituted oxotriazinoindoles was developed with the aim to investigate molecular interactions within the aldose reductase (ALR2) inhibitor binding site. About twice increased inhibition efficacy of the most efficient derivative **14** (*N(2)*-CH_2CH_2COOH) compared to the unsubstituted lead **OTI** was obtained, yet at the expense of selectivity relative to anti-target aldehyde reductase (ALR1). To explain the major drop in selectivity, observed also in other *N(2)*-substituted derivatives, *in silico* molecular modeling approach revealed the role of extra interactions with the residues of Arg309, Arg312 and Met302 located in the additional *C*-terminal loop of ALR1 missing in ALR2, which can prevent or enhance binding in ALR1. These key findings will be used for development of the next generation of selective OTI inhibitors.

1. Computational Methods.

The initial structures of compounds were calculated by the equilibrium conformer search procedure (MMFF94) in the program SPARTAN'08 (Wavefunction, Inc., Irvine, CA, 2009). The geometries of individual tautomers for compound **OTI** (tautomers analogical to those calculated for compound cemtirestat (**CMTI**) in the paper of Stefek et al., 2015) were obtained by full optimization in the DFT B3LYP 6-31G* method in vacuum, in water, and in DMSO. The energies of solvated tautomers in water and in DMSO were calculated by the SM8 method of Cramer and Truhlar et al., 2007. The structure of human recombinant enzyme AKR1B1 in the complex with $NADP^+$ and cemtirestat (**CMTI**) (PDB: 4QX4) was used for docking (Stefek et al., 2015). The optimal conformers of the inhibitors were docked into the enzyme-cofactor complex by the program Yasara (Krieger et al., 2014) using the AMBER14 force field (Maier et al., 2015) and utilizing the flexible ligands option. The first five clusters (if existing) as ordered by AutoDock binding energy were then optimized in water. The simulation cell overlapping the complex by 8 Å was filled by water molecules (final density 0.997 g/ mL) and Na^+ and Cl^- ions in the amount of 0.9 % of the overall mass of the water environment. The ratio of the ions was chosen to neutralize the final charge of the complex. Recalculation of pKa values of amino acids was performed and pH 6.2 was maintained (Krieger et al., 2006). A standard optimization protocol, which consists of the steepest gradient optimization, molecular dynamics and simulated annealing, was used. The rational geometry with the highest binding energy (according to Yasara convention) was chosen for analysis of the key interactions. To validate the protocol, a cross-docking procedure was performed and confirmed a high value of accuracy of 90.0 % (Majekova et al., 2017). In order to compare the complexes with compound **OTI** and with cemtirestat (**CMTI**), the original PDB: 4QX4 structure was relaxed with the same optimization protocol.

2. Chemistry. Starting chemicals for syntheses were purchased from Sigma-Aldrich (St. Louis, MO, USA), Fluorochem (Hadfield, UK), AlfaAesar (part of Thermo Fisher Scientific, Heysham, UK), or Acros (part of Thermo Fisher Scientific, Geel, Belgium) vendors. Other chemicals were purchased from local commercial sources and were of analytical grade quality. Melting points were measured by a Digital Melting Point Apparatus Barnstead Electrothermal IA9200 and are uncorrected. ^{1}H- and ^{13}C NMR spectra were recorded on Varian Gemini (600 and 150 MHz, resp.); chemical shifts are given in parts per million (ppm), and tetramethylsilane was used as an internal standard and DMSO-d6 as the solvent, unless otherwise specified. Infrared (IR) spectra were acquired on Fourier transform infrared spectroscopy (FT-IR)-attenuated total reflectance REACT IR 1000 (ASI Applied Systems) with a diamond probe and MTS detector. Mass spectra were performed on liquid chromatography-mass spectrometry (LC-MS; Agilent Technologies 1200 Series equipped with Mass spectrometer Agilent Technologies 6100 Quadrupole LC-MS). The course of the reactions was followed by thin-layer chromatography (TLC) analysis (Merck Silica gel 60 F254). A UV lamp (254 nm) and iodine vapours were used for the visualization of TLC spots. All tested compounds **5**, **8**, **11** and **14** possess purity over 95%. Their purity was determined by the melting point and combustion analysis (elemental analysis found values for carbon, hydrogen, and nitrogen within 0.4% of the calculated values for the proposed formula).

Ethyl 2-(3-oxo-2,3-dihydro-5*H*-[1,2,4]triazino[5,6-*b*]indol-5-yl)acetate (2)

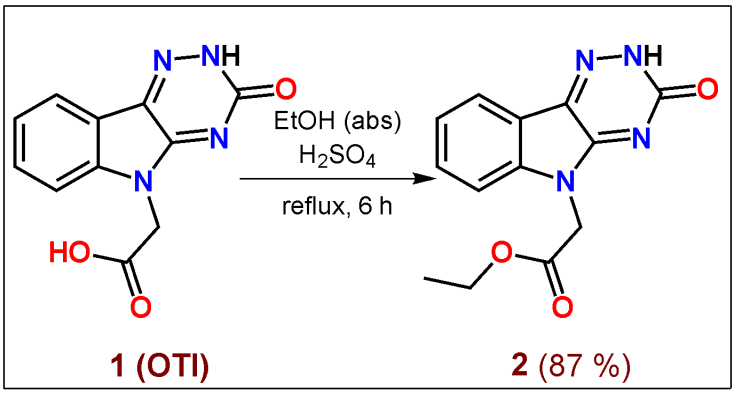

To a solution of 1.00 g (4.10 mmol, 1.00 mol eq) **1** (**OTI**) in 100 mL of EtOH (abs), 2.00 mL (3.66 g, 37.3 mmol, 9.10 mol eq) of H_2SO_4 (conc, d: 1.83 g/ml) was added. Reaction mixture was refluxed at 100 °C for 6 h. Completion of the reaction was analysed by TLC (SiO_2, MeOH / EA, 1 / 1). A solvent was evaporated by RVE and obtained crude mixture dissolved in 150 mL of $CHCl_3$ and washed with water. Combined organic layer was extracted with water, aq solution of Na_2CO_3 and dried by standing over Na_2SO_4. After filtration, product **7** was isolated by RVO evaporation and dried under reduced pressure to yield 966 mg (3.55 mmol, 87 %).

Novelty: Compound **2** was described by our recent publication with ^{1}H-, ^{13}C-NMR, IR and MS spectra.[5]

Melting point: 247.0 - 254.0 °C [$CHCl_3$] (lit. 248.0 - 252.0 °C).

^{1}H-NMR diagram:

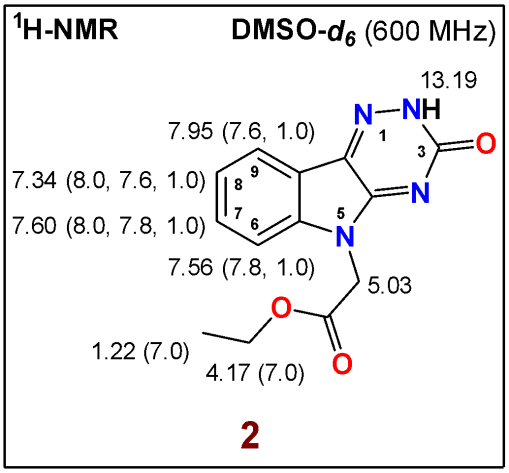

^{1}H-NMR (600 MHz, DMSO-d_6): δ 13.19 (br s, 1H, -N<u>H</u>-); 7.95 (dd, 1H, *J(8,9)* = 7.6 Hz, *J(7,9)* = 1.0 Hz, H-C(9)); 7.60 (ddd, 1H, *J(7,8)* = 8.0 Hz, *J(6,7)* = 7.80 Hz, *J(7,9)* = 1.0 Hz, H-C(7)); 7.56 (dd, 1H, *J(6,7)* = 7.8 Hz, *J(6,8)* = 1.0 Hz, H-C(6)); 7.34 (ddd, 1H, *J(7,8)* = 8.0 Hz, *J(8,9)* = 7.6 Hz, *J(6,8)* = 1.0 Hz, H-C(8)); 5.03 (s, 2H, -NC<u>H</u>$_2$COOEt); 4.17 (q, 2H, *J*(CH_2,CH_3) = 7.0 Hz, -OC<u>H</u>$_2$$CH_3$); 1.22 (t, 3H, *J*($CH_2$,$CH_3$) = 7.0 Hz, -OCH$_2$C<u>H</u>$_3$).

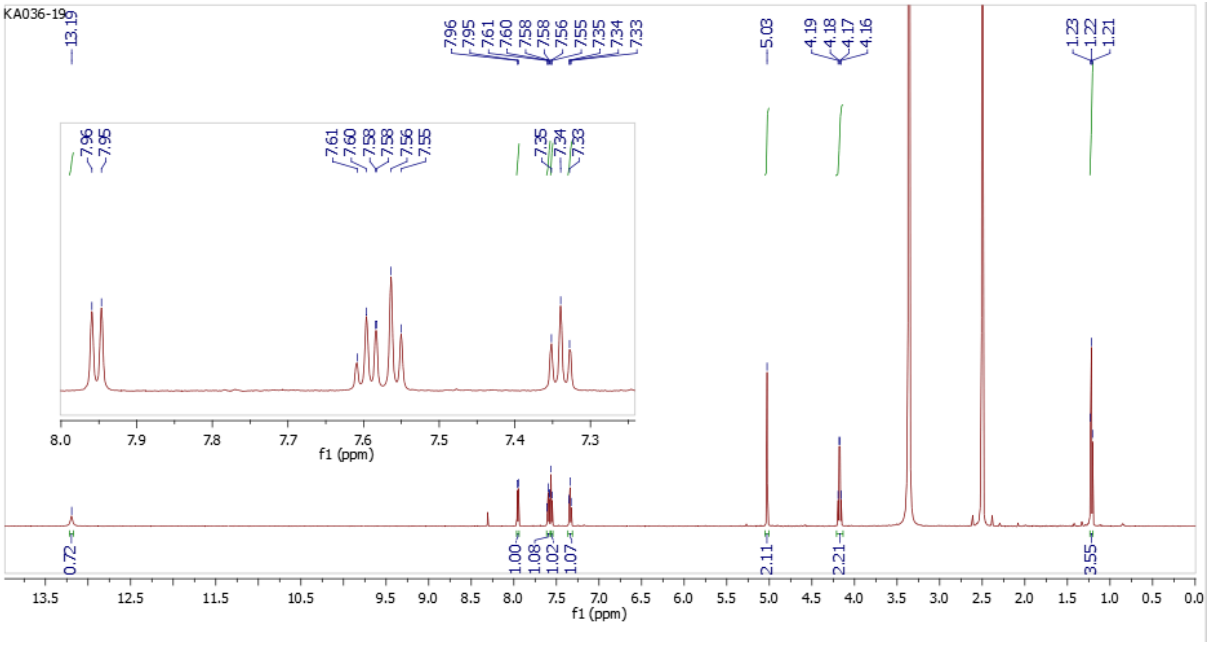

Figure 7. ^{1}H-NMR (600 MHz, DMSO-d_6) spectrum of compound **2**.

Ethyl 2-(3-oxo-2,3-dihydro-5*H*-[1,2,4]triazino[5,6-*b*]indol-5-yl)acetate (4)**.**

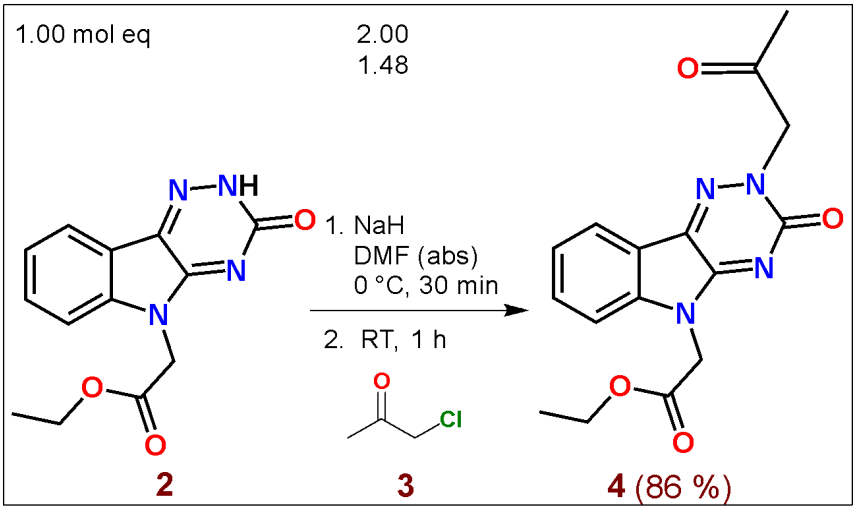

Ethyl ester **2** 200 mg (0.73 mmol, 1.00 mol eq) of was dissolved in 1.5 mL of DMS (abs) and deprotonated by 35.2 mg (1.47 mmol, 2.00 mol eq) of NaH. The reaction was stirred at 0 °C within 30 min. Afterwards 87.2 µL (100 mg, 1.08 mmol, 1.48 mol eq) of chloroacetone (**3**) (d: 1.15 g/mL) was added and the mixture stirred at RT for 1 h. TLC analysis (SiO_2, Hex / EA, 1 / 5) confirmed complete conversion of **2** to a novel compound. Then, the mixture was extracted with EA (3 x 30 mL). Combined organic layer was washed with brine (5 x 50 mL) and dried by standing over Na_2SO_4. After filtration and RVE evaporation, product **4** was dried under high vacuum to yield 206 mg (0.63 mmol, 86 %) of yellow solid compound.

Novelty: Compound **4** was not yet described in literature.

Melting point: 177.8 - 184.4 °C [EA].

NMR diagrams:

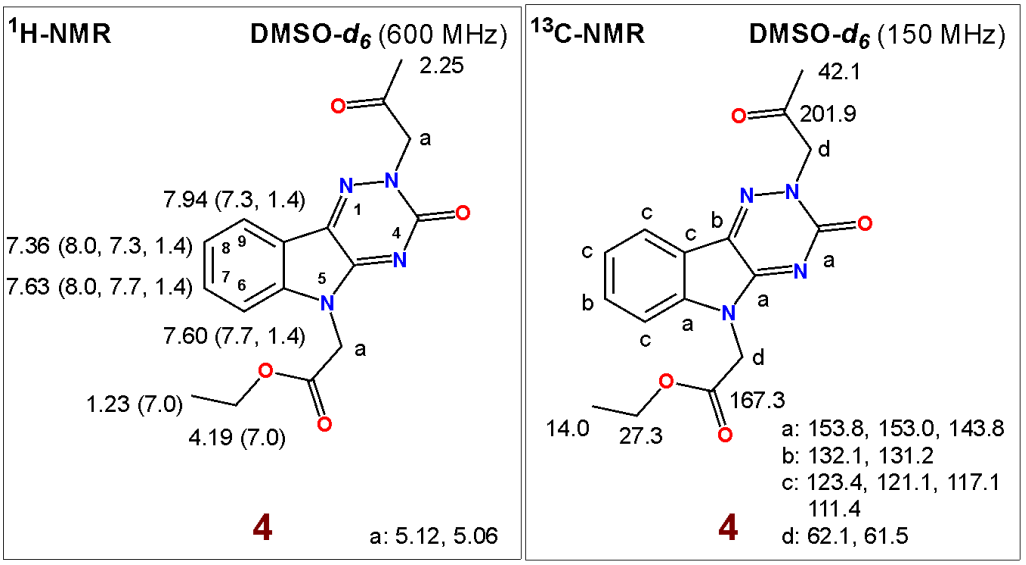

^{1}H-NMR (600 MHz, DMSO-d_6): δ 7.94 (dd, 1H, J(8,9) = 7.3 Hz, J(7,9) = 1.4 Hz, H-C(9)), 7.63 (ddd, 1H, J(7,8) = 8.0 Hz, J(6,7) = 7.7 Hz, J(7,9) = 1.4 Hz, H-C(7)), 7.60 (dd, 1H, J(6,7) = 7.7 Hz, J(6,8) = 1.4 Hz, H-C(6)), 7.36 (ddd, 1H, J(7,8) = 8.0 Hz, J(8,9) = 7.3 Hz, J(6,8) = 1.4 Hz, H-C(8)), 5.12 and 5.06 (2 x s, 2 x 2H, -C$\underline{H}_2$COOEt and -C$\underline{H}_2$COCH$_3$), 4.19 (q, 2H, J(CH$_2$,CH$_3$) = 7.0 Hz, -COOC$\underline{H}_2$CH$_3$), 2.25 (s, 3H, -CH$_2$OC$\underline{H}_3$), 1.23 (t, 3H, J(CH$_2$,CH$_3$) = 7.0 Hz, -COOCH$_2$C$\underline{H}_3$).

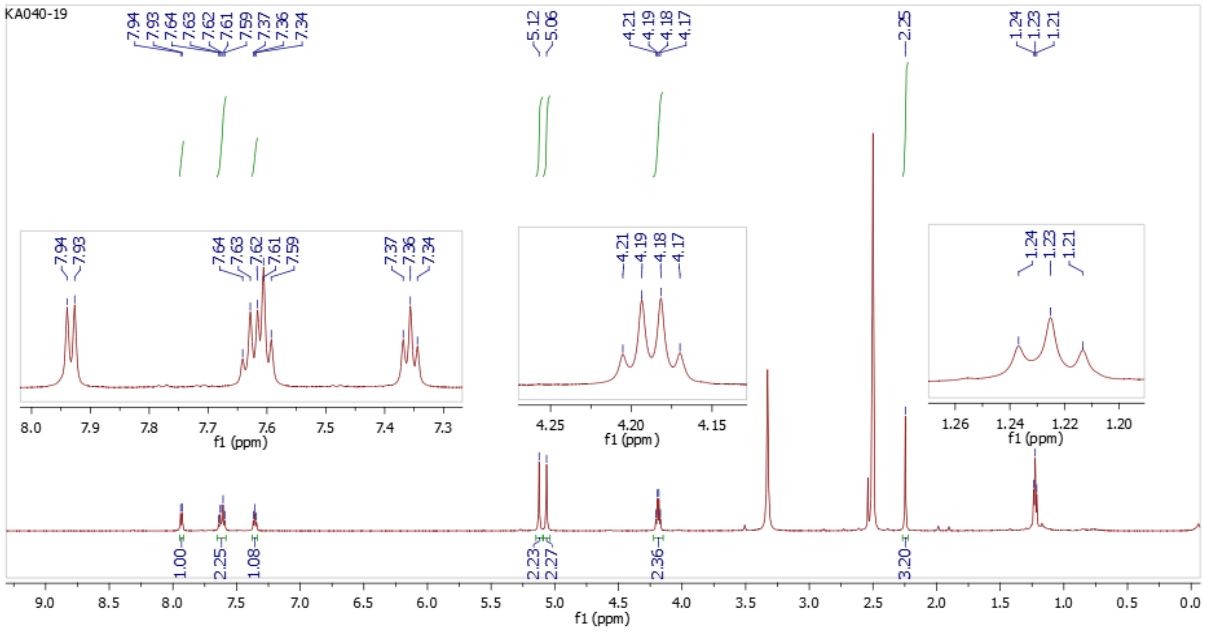

Figure 8. ^{1}H-NMR (600 MHz, DMSO-d_6) spectrum of compound **4**.

^{13}C-NMR (150 MHz, DMSO-d_6): δ 201.9 (-CH$_2$$\underline{C}OCH_3$), 167.3 (-CH$_2$-$\underline{C}$OOEt), 153.8, 153.0, 143.8, 132.1, 131.2, 123.4, 121.1, 117.1, 111.4, 62.1, 61.5 (-CH$_2$CO$\underline{C}$H$_3$), 42.1, 27.3 (-COCH$_3$), 14.0 (-OCH$_2$$\underline{C}H_3$).

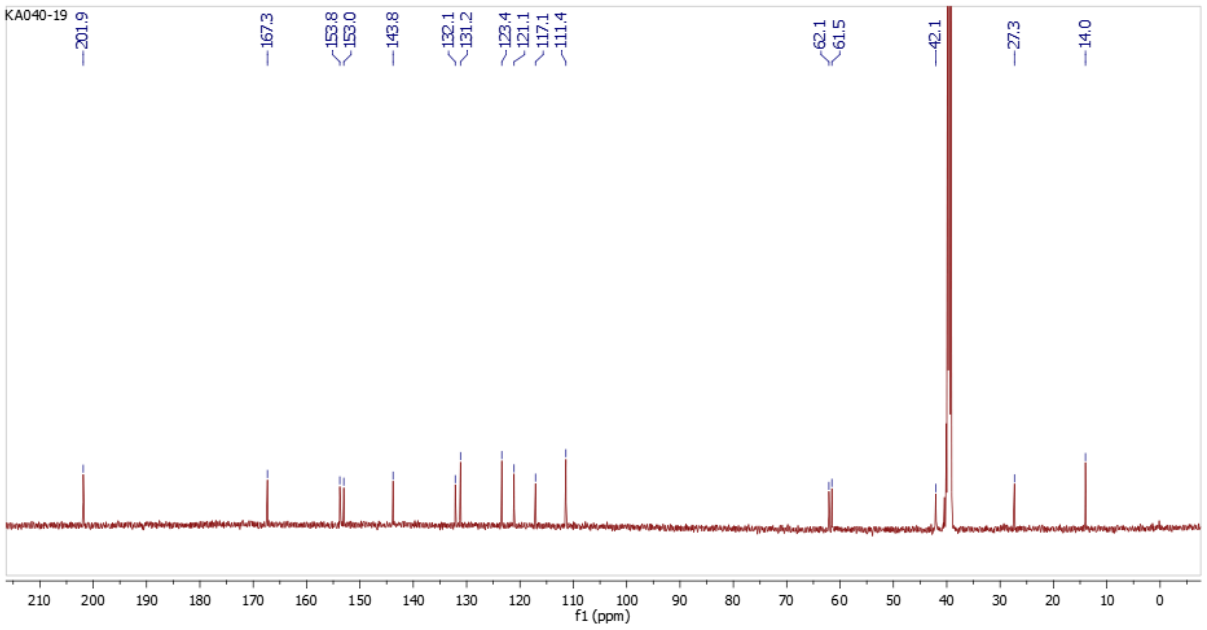

Figure 9. ^{13}C-NMR (150 MHz, DMSO-d_6) spectrum of compound **4**.

FT-IR (solid, cm^{-1}): 2605 (w), 2345 (w), 1733 (s), 1690 (s), 1602 (s), 1569 (s), 1503 (m), 1470 (m), 1400 (s), 1339 (s), 1275 (s), 1231 (s), 1142 (m), 1001 (m), 941 (m), 895 (m), 789 (m), 751 (s), 700 (m), 646 (m), 607 (m), 549 (m), 513 (m), 439 (s).

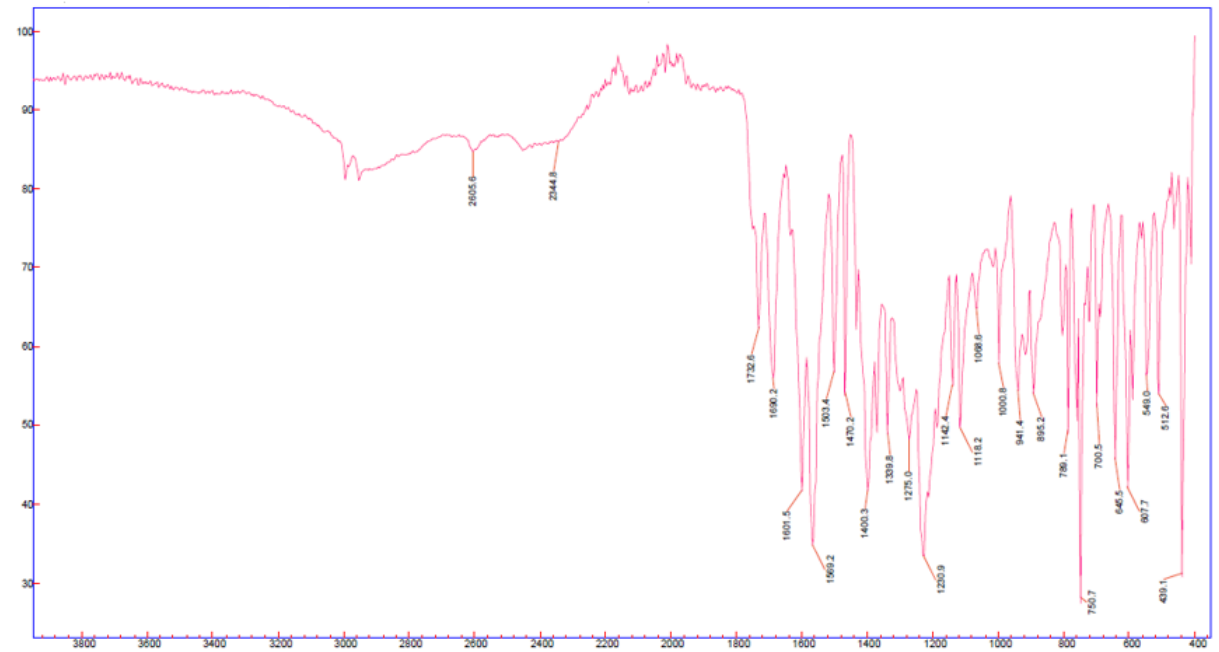

Figure 10. FT-IR (solid, cm^{-1}) spectrum of compound **4**.

MS (ESI m/z, positive ion mode): 329.0 $[M+H]^+$.

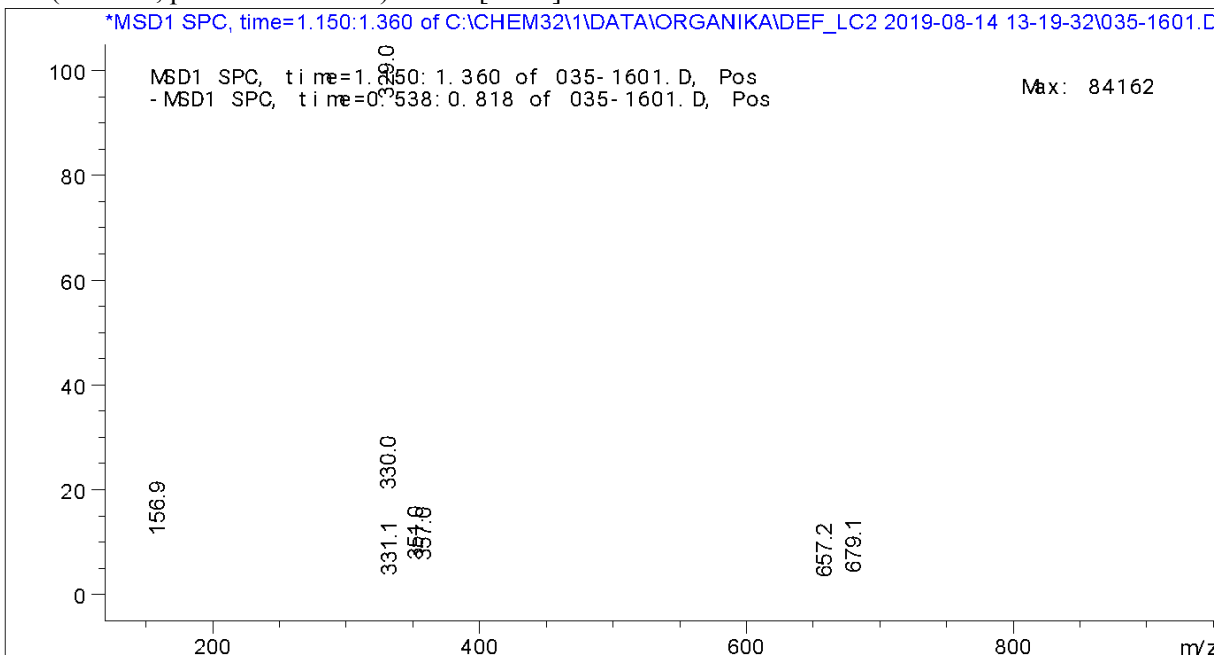

Figure 11. MS (ESI m/z, positive ion mode) spectrum of compound **4**.

Elemental analysis. Anal. Calcd for $C_{16}H_{16}N_4O_4$ (326.12): C, 58.53; H, 4.91; N, 17.06; found: C, 58.62; H, 5.02; N, 17.15.

2-(3-Oxo-2-(2-oxopropyl)-2,3-dihydro-5*H*-[1,2,4]triazino[5,6-*b*]indol-5-yl)acetic acid (5)**.**

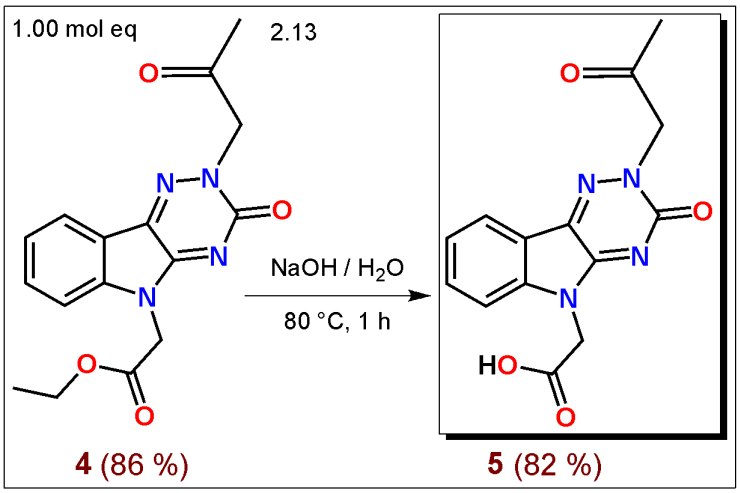

Ethyl ester **4** 20.0 mg (0.061 mmol, 1.00 mol eq) was dissolved in aqueous solution 5.10 mg (0.128 mmol, 2.13 mol eq) of NaOH. Reaction mixture was stirred at 80° C for 1 h. Complete conversion of **4** was confirmed by TLC analysis (SiO_2, MeOH / EA = 1 / 1). Afterwards the mixture was cooled down in an ice bath and acidified with 1M aq HCl solution to pH = 2. Obtained precipitate (product **5**) was filtered off and purified by crystallisation from a mixture of H_2O / DMSO. Yellow crystals were isolated by filtration and dried under reduced pressure to yield 15.0 mg (0.050 mmol, 82 %) of compound **5**.

Novelty: Compound **5** was not yet described in the literature.

Melting point: 259.1 - 264.8 °C [H_2O / DMSO].

NMR diagrams:

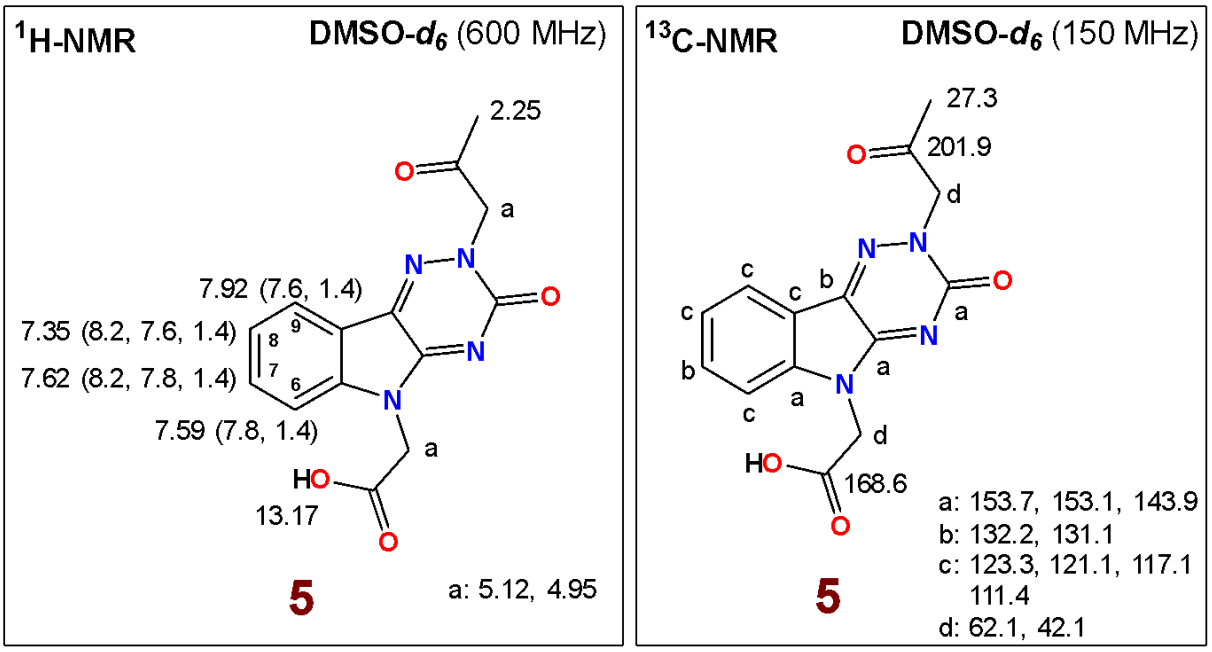

^{1}H-NMR (600 MHz, DMSO-d_6): δ 13.17 (br s, 1H, -COOH), 7.92 (dd, 1H, J(8,9) = 7.6 Hz, J(7,9) = 1.4 Hz, H-C(9)), 7.62 (ddd, 1H, J(7,8) = 8.2 Hz, J(6,7) = 7.8 Hz, J(7,9) = 1.4 Hz, H-C(7)), 7.59 (dd, 1H, J(6,7) = 7.8 Hz, J(6,8) = 1.4 Hz, H-C(6)), 7.35 (ddd, 1H, J(7,8) = 8.2 Hz, J(8,9) = 7.6 Hz, J(6,8) = 1.4 Hz, H-C(8)), 5.12 and 4.95 (2 x s, 2 x 2H, -CH_2COOEt and -CH_2COCH$_3$), 2.25 (s, 3H, -CH$_2$COCH_3).

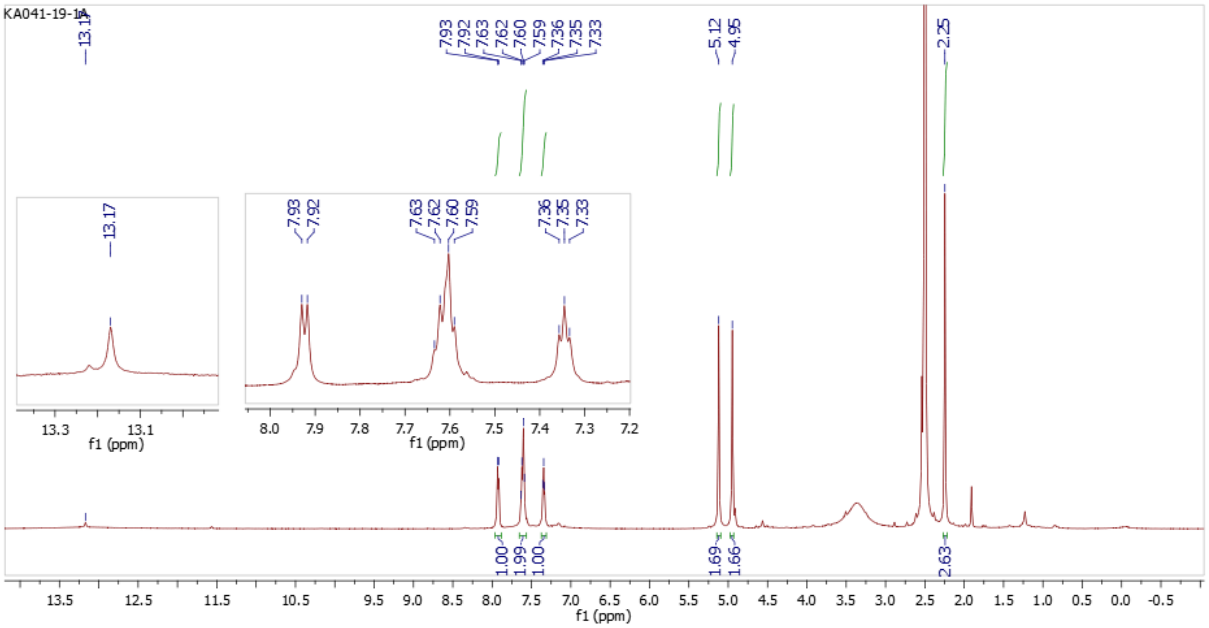

Figure 12. ^{1}H-NMR (600 MHz, DMSO-d_6) spectrum of compound **5**.

^{13}C-NMR (150 MHz, DMSO-d_6): δ 201.9 (-CH$_2$COCH$_3$), 168.6 (-CH$_2$COOH), 153.7, 153.1, 143.9, 132.2, 131.1, 123.3, 121.1, 117.1, 111.4, 62.1, 42.1, 27.3 (-CH$_2$COCH$_3$).

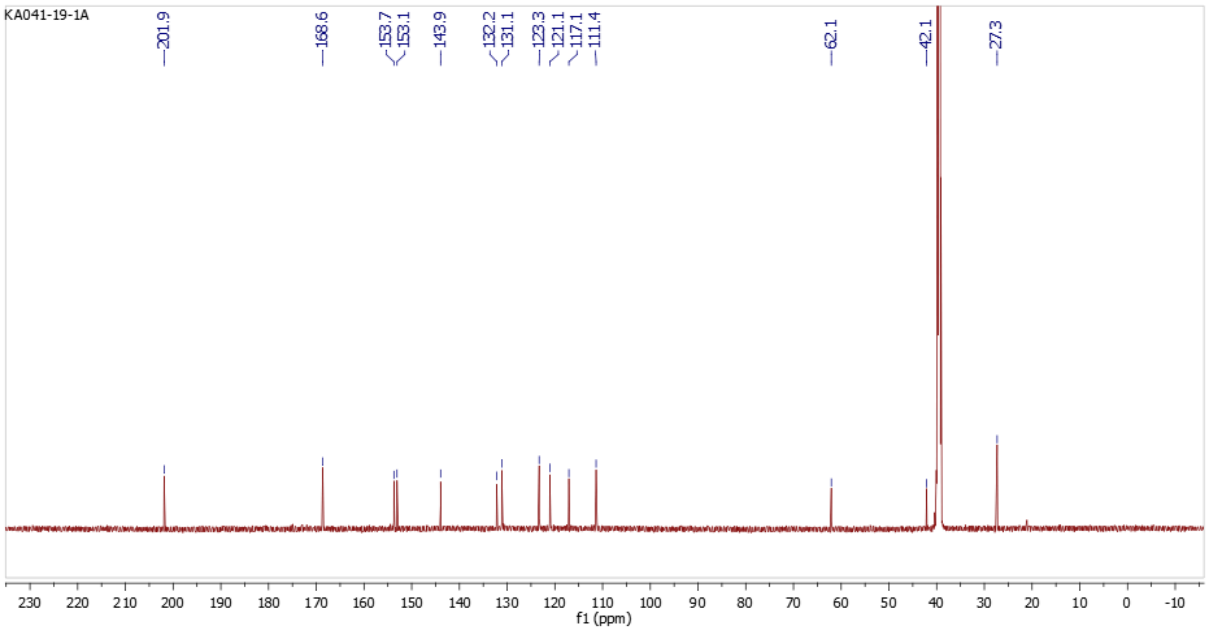

Figure 13. ^{13}C-NMR (150 MHz, DMSO-d_6) spectrum of compound **5**.

FT-IR (solid, cm^{-1}): 3245 - 2080 (br, =CH-, -CH- and -COOH), 1740 (s), 1608 (s), 1575 (s), 1501 (s), 1465 (s), 1412 (s), 1370 (m), 1268 (m), 1218 (s), 1166 (s), 1088 (s), 1005 (s), 914 (s), 892 (m), 787 (s), 748 (s), 671 (m).

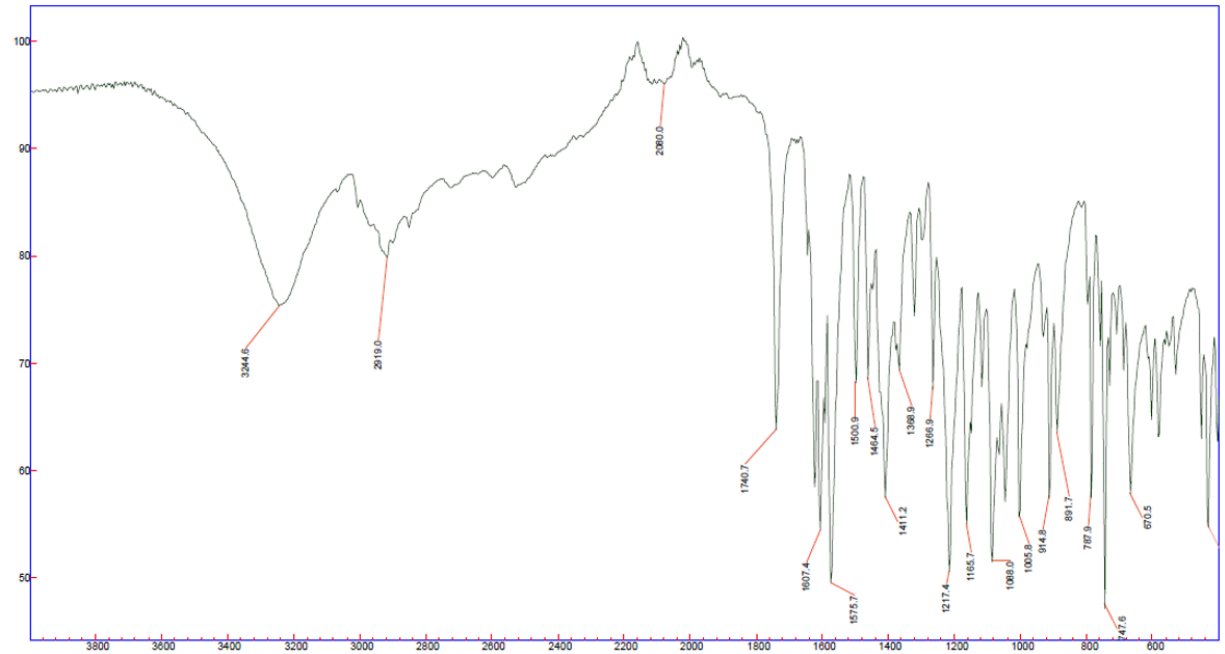

Figure 14. FT-IR (solid, cm^{-1}) spectrum of compound **5**.

MS (ESI m/z, negative ion mode): 299.0 (32 %) $[M-H]^+$, 255.1 (67 %) $[M-CO_2-H]^+$.

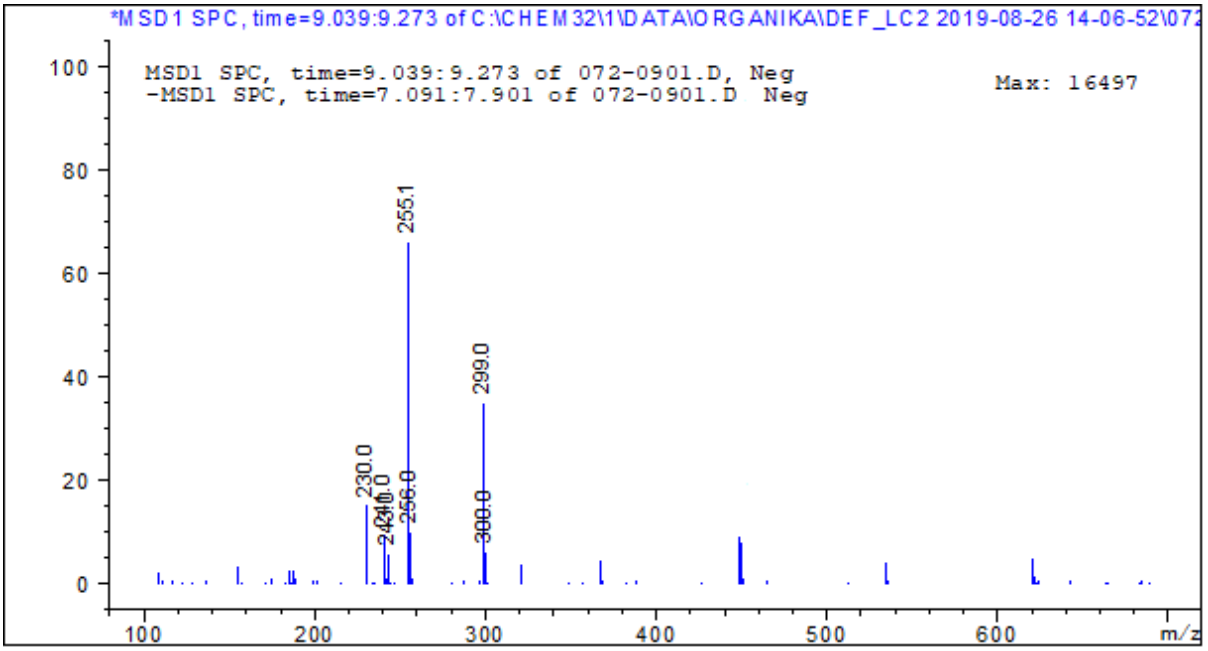

Figure 15. MS (ESI m/z, negative ion mode) spectrum of compound **5**.

Elemental analysis. Anal. Calcd for $C_{14}H_{12}N_4O_4$ (300.27): C, 56.00; H, 4.03; N, 18.66; found: C, 56.31; H, 4.30; N, 18.45.

Ethyl 2-(2-(2-acetoxyethyl)-3-oxo-2,3-dihydro-5*H*-[1,2,4]triazino[5,6-*b*]indol-5-yl)acetate (7)

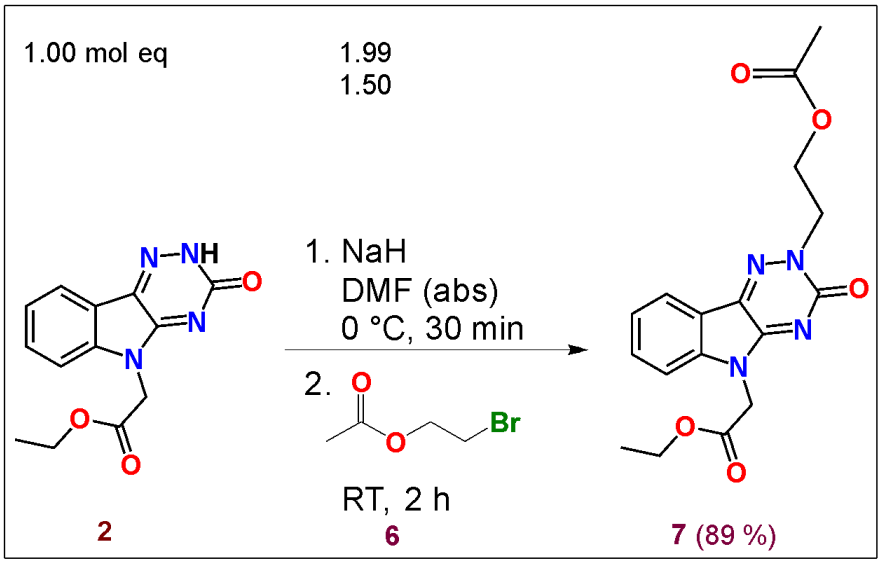

Ethyl ester **2** 100.0 mg (0.37 mmol, 1.00 mol eq) was dissolved in 1.5 mL of DMF (abs) and deprotonated by 17.7 mg (0.74 mmol, 1.99 mol eq) of NaH. The reaction was stirred at 0 °C within 30 min. Afterwards 61 µL (92.68 mg, 0.56 mmol, 1.50 mol eq) of 2-bromoethyl acetate (**6**) (d: 1.51 g/mL) was added and the mixture stirred at RT °C for 2 h. TLC analysis (SiO_2, Hex / EA, 1 / 5) confirmed complete conversion of **2** to a novel compound. Then, the mixture was extracted with EA (3 x 30 mL). Combined organic layer was washed with brine (5 x 50 mL) and separated organic phase dried by standing over Na_2SO_4. After filtration and RVE evaporation, product **7** was dried under high vacuum to yield 117 mg (0.33 mmol, 89 %) of yellow solid compound.
Novelty: Compound **7** was not yet described in the literature.

Melting point: 85.0 - 89.5 °C [EA].
NMR diagrams:

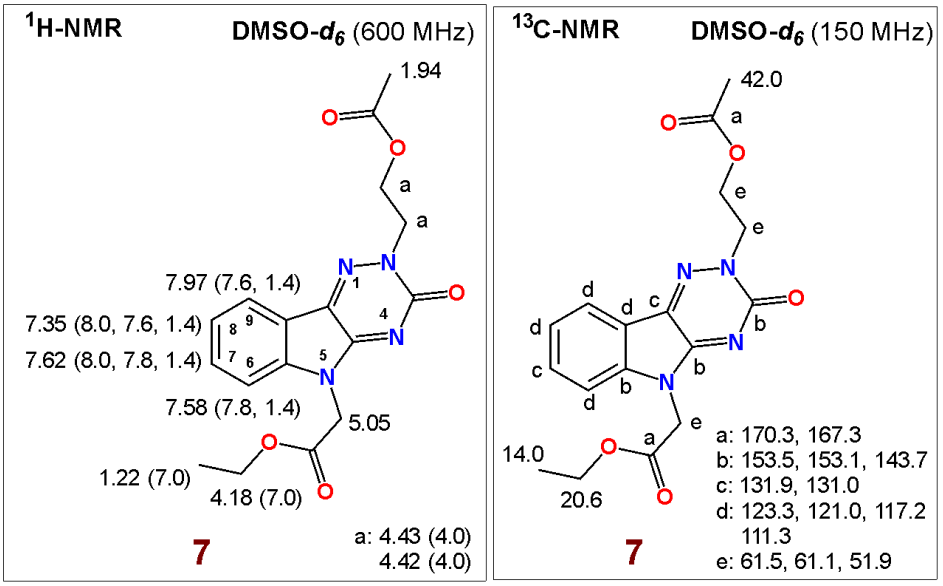

^{1}H-NMR (600 MHz, DMSO-d_6): δ 7.97 (dd, 1H, J(8,9) = 7.6 Hz, J(7,9) = 1.4 Hz, H-C(9)), 7.62 (ddd, 1H, J(7,8) = 8.0 Hz, J(6,7) = 7.8 Hz, J(7,9) = 1.4 Hz, H-C(7)), 7.58 (dd, 1H, J(6,7) = 7.8 Hz, J(6,8) = 1.4 Hz, H-C(6)), 7.35 (ddd, 1H, J(7,8) = 8.0 Hz, J(8,9) = 7.6 Hz, J(6,8) = 1.4 Hz, H-C(8)), 5.05 (s, 2H, -C$\underline{H}_2$-N(5)), 4.43 and 4.42 (2 x s, 2 x 2H, -C$\underline{H}_2$CH$_2$OCOCH$_3$ and -CH$_2$C$\underline{H}_2$OCOCH$_3$), 4.18 (q, 2H, J(CH$_2$,CH$_3$) = 7.0 Hz, -OC$\underline{H}_2$CH$_3$), 1.94 (s, 3H, -OCOC$\underline{H}_3$), 1.22 (t, 3H, J(CH$_2$,CH$_3$) = 7.0 Hz, -OCH$_2$C$\underline{H}_3$).

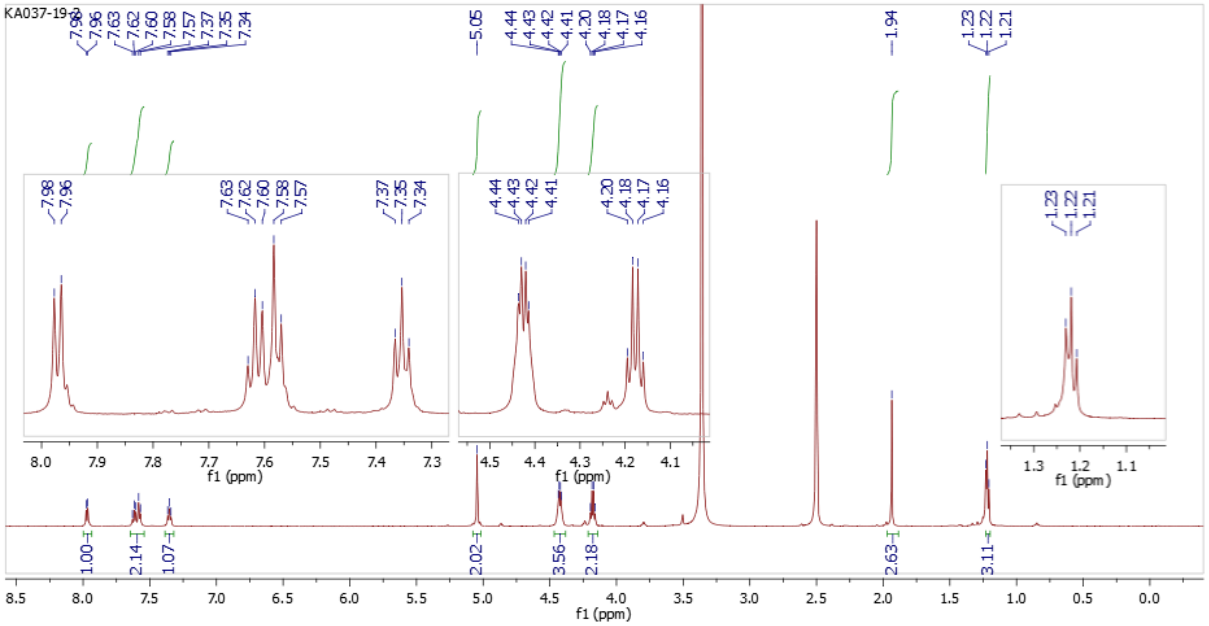

Figure 16. ^{1}H-NMR (600 MHz, DMSO-d_6) spectrum of compound **7**.

^{13}C-NMR: (150 MHz, DMSO-d_6): δ 170.3, 167.3, 153.5, 153.1, 143.7, 131.9, 131.0, 123.3, 121.0, 117.2, 111.3, 61.5 (-O$\underline{C}$H$_2$CH$_3$), 61.1, 51.9, 42.0, 20.6 (-OCO$\underline{C}$H$_3$), 14.0 (-OCH$_2\underline{C}$H$_3$).

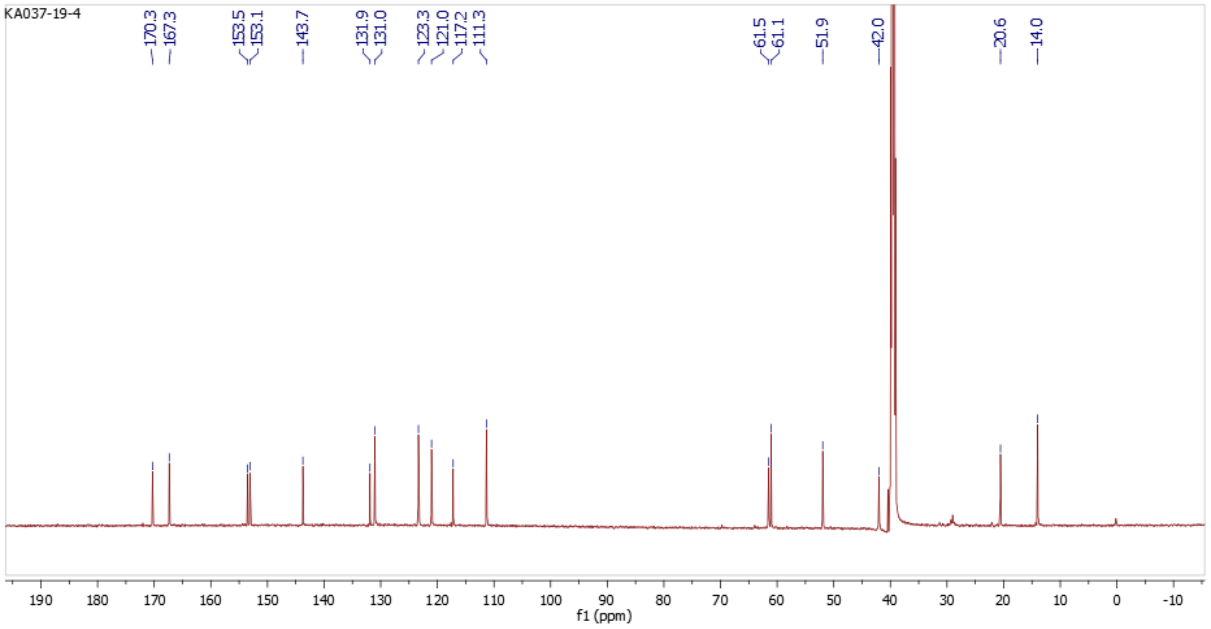

Figure 17. ^{13}C- NMR (150 MHz, DMSO-d_6) spectrum of compound **7**.

FT-IR (solid, cm^{-1}): 1735 (s), 1684 (s), 1604 (s). 1576 (m), 1464 (s), 1420 (m), 1375 (s), 1274 (m), 1194 (s), 1108 (s), 1020 (m), 961 (m), 870 (m), 786 (s), 745 (s), 567 (m), 470 (s).

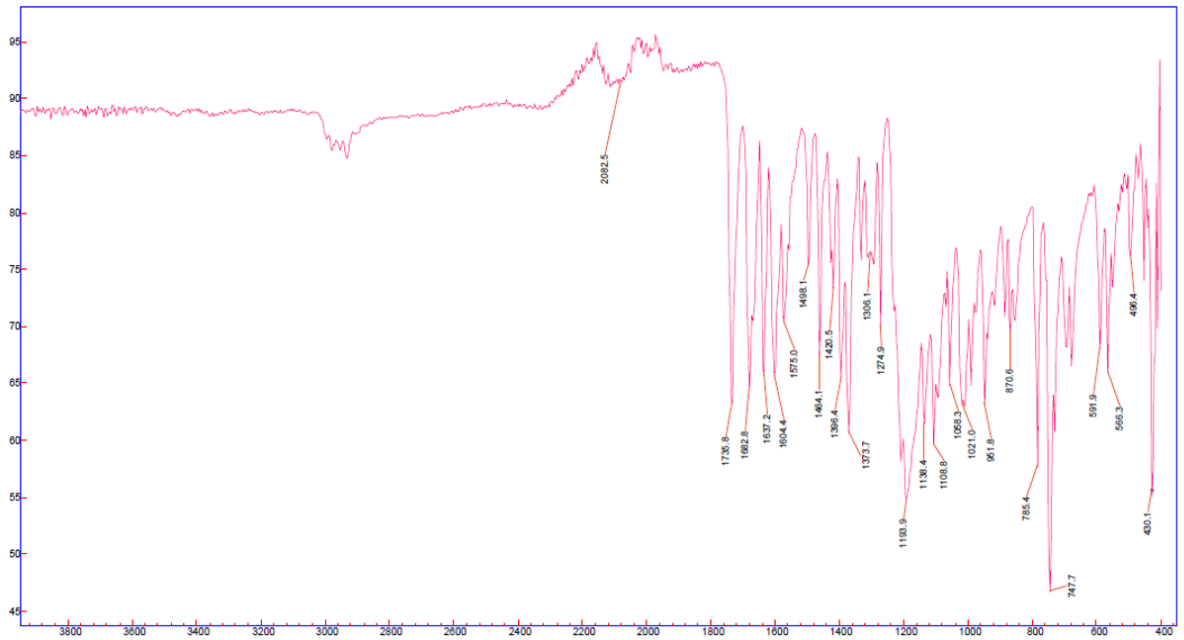

Figure 18. FT-IR (solid, cm^{-1}) spectrum of compound **7**.

MS (ESI m/z, positive ion mode): 359.1 $[M+H]^+$.

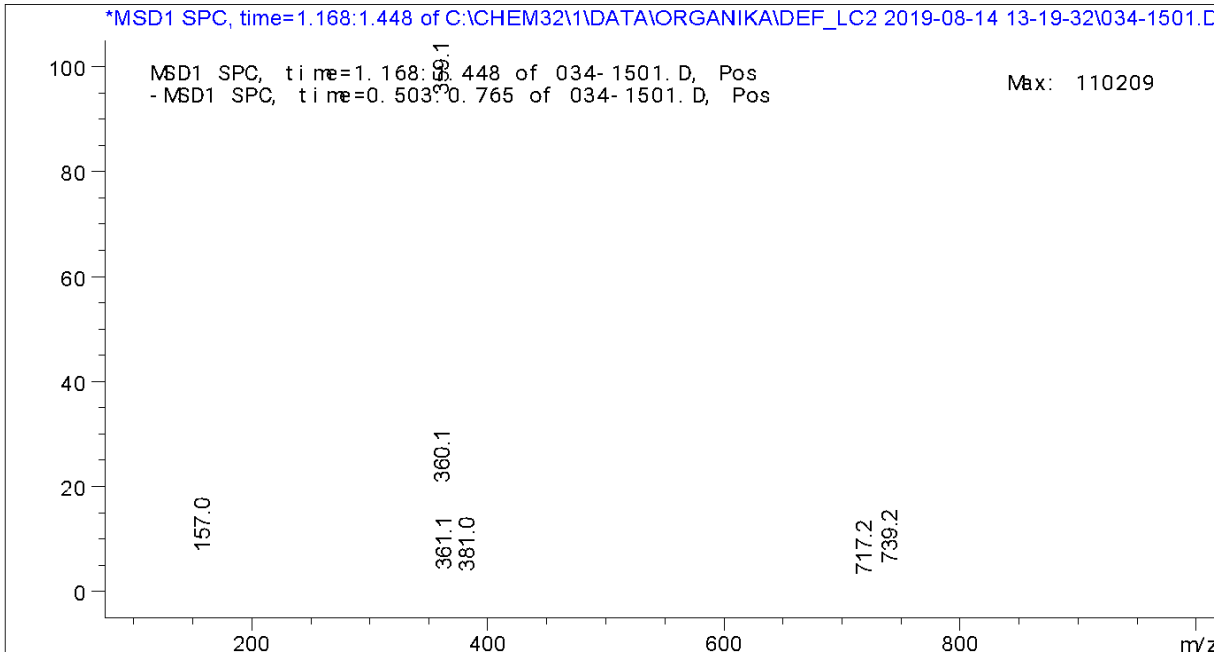

Figure 19. MS (ESI m/z, positive ion mode) spectrum of compound **7**.

Elemental analysis. Anal. Calc for $C_{17}H_{18}N_4O_5$ (358.35): C, 56.98; H, 5.06; N, 15.63; O, 22.32; found: C, 56.83; H, 5.12; N, 15.55.

Ethyl 2-(2-(2-acetoxyethyl)-3-oxo-2,3-dihydro-5*H*-[1,2,4]triazino[5,6-*b*]indol-5-yl)acetate

(8)

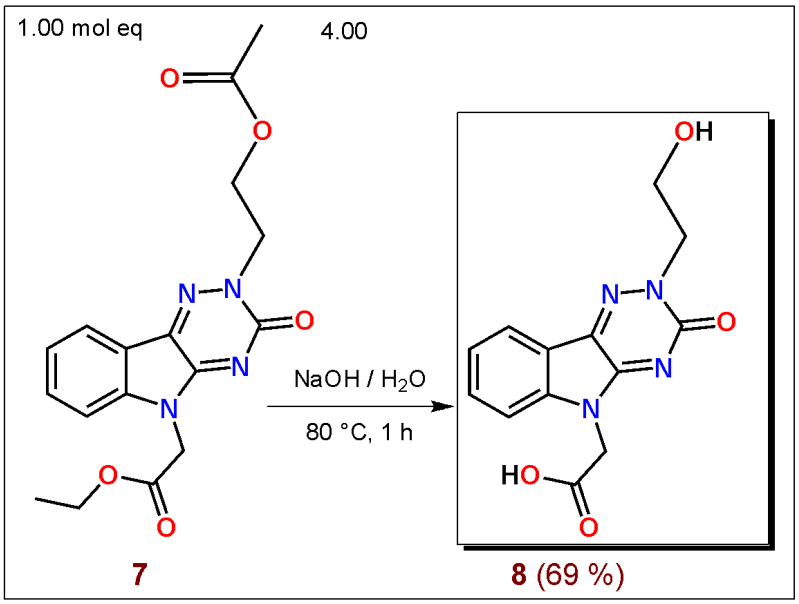

Ethyl ester **7** 100.0 mg (0.28 mmol, 1.00 mol eq) was dissolved in an aqueous solution prepared from 44.8 mg (1.12 mmol, 4.00 mol eq) NaOH in 100 mL of H_2O. The reaction mixture was stirred at 80 °C for 1 h. Complete conversion of **7** was confirmed by TLC analysis (SiO_2, MeOH / EA = 1 / 1). Afterwards the mixture was cooled down in an ice bath and acidified by 1 M HCl aq solution to pH 2. Formed precipitate of product **8** was filtered off and purified by crystallisation from a mixture of H_2O / DMSO. Yellow crystals were isolated by filtration and dried under high vacuum to yield 55.7 mg (0.19 mmol, 69 %) of compound **8**.

Novelty: Compound **8** was not yet described in the literature.
Melting point: 256.4 - 260.7 °C [H_2O / DMSO].
NMR diagrams:

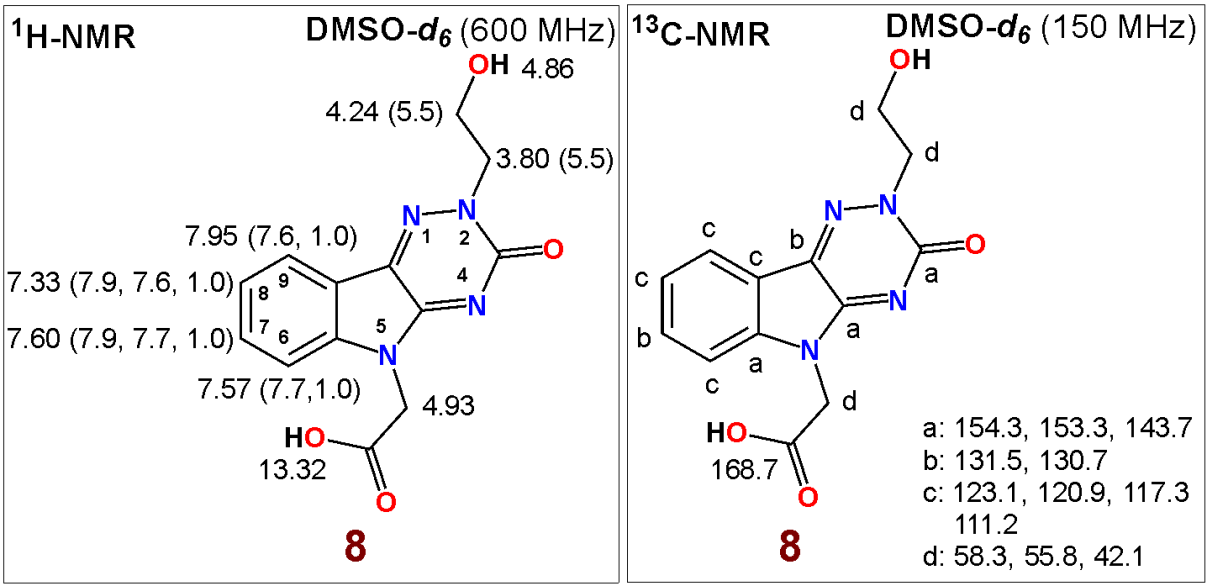

^{1}H-NMR (600 MHz, DMSO-d_6): δ 13.32 (br s, 1H, -CH_2COO<u>H</u>), 7.95 (dd, 1H, J(8,9) = 7.6 Hz, J(7,9) = 1.0 Hz, H-C(9)), 7.60 (ddd, 1H, J(7,8) = 7.9 Hz, J(6,7) = 7.7 Hz, J(7,9) = 1.0 Hz, H-C(7)), 7.57 (dd, 1H, J(6,7) = 7.7 Hz, J(6,8) = 1.0 Hz, H-C(6)), 7.33 (ddd, 1H, J(7,8) = 7.9 Hz, J(8,9) = 7.6 Hz, J(6,8) = 1.0 Hz, H-C(8)), 4.93 (s, 2H, -C<u>H_2</u>-N(5)), 4.86 (br s, 1H, -CH_2CH_2O<u>H</u>), 4.24 (t, 2H, J(CH_2,CH_3) = 5.5 Hz, -N(2)CH_2C<u>H_2</u>OH), 3.80 (t, 2H, J(CH_2,CH_3) = 5.5 Hz, -N(2)C<u>H_2</u>CH_2OH).

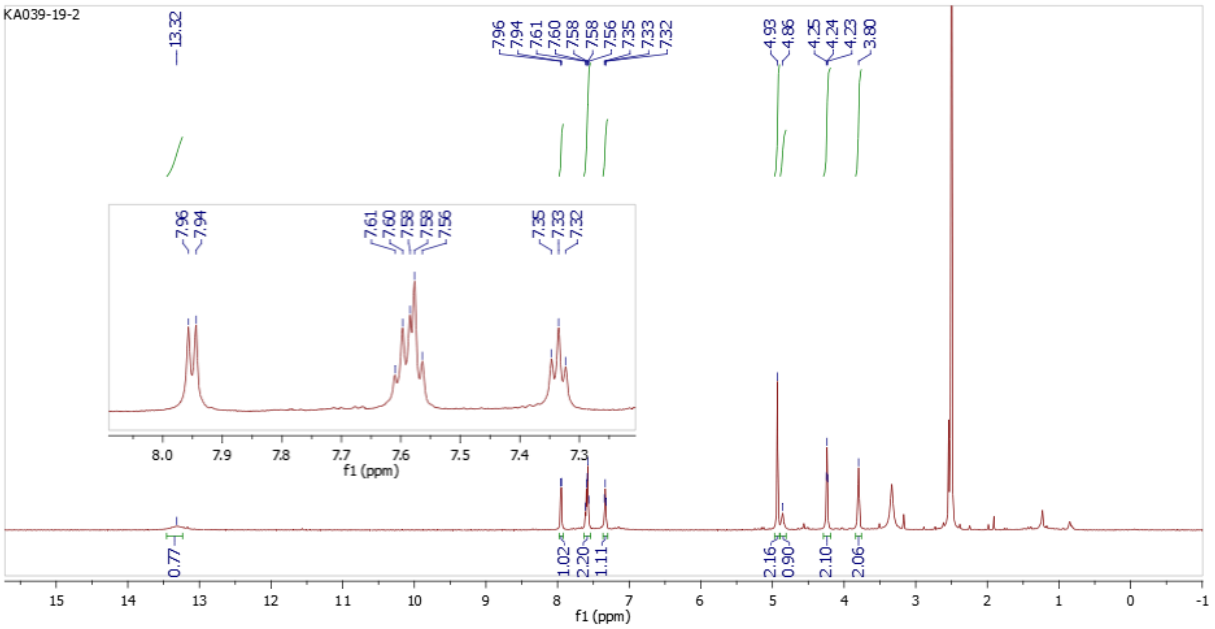

Figure 20. ^{1}H-NMR (600 MHz, DMSO-d_6) spectrum of compound **8**.

^{13}C-NMR (150 MHz, DMSO-d_6): δ 168.7 (-NCH_2<u>C</u>OOH), 153.4, 153.3, 143.7, 131.5, 130.7, 123.1, 120.9, 117.3, 111.2, 58.3, 55.8, 42.0.

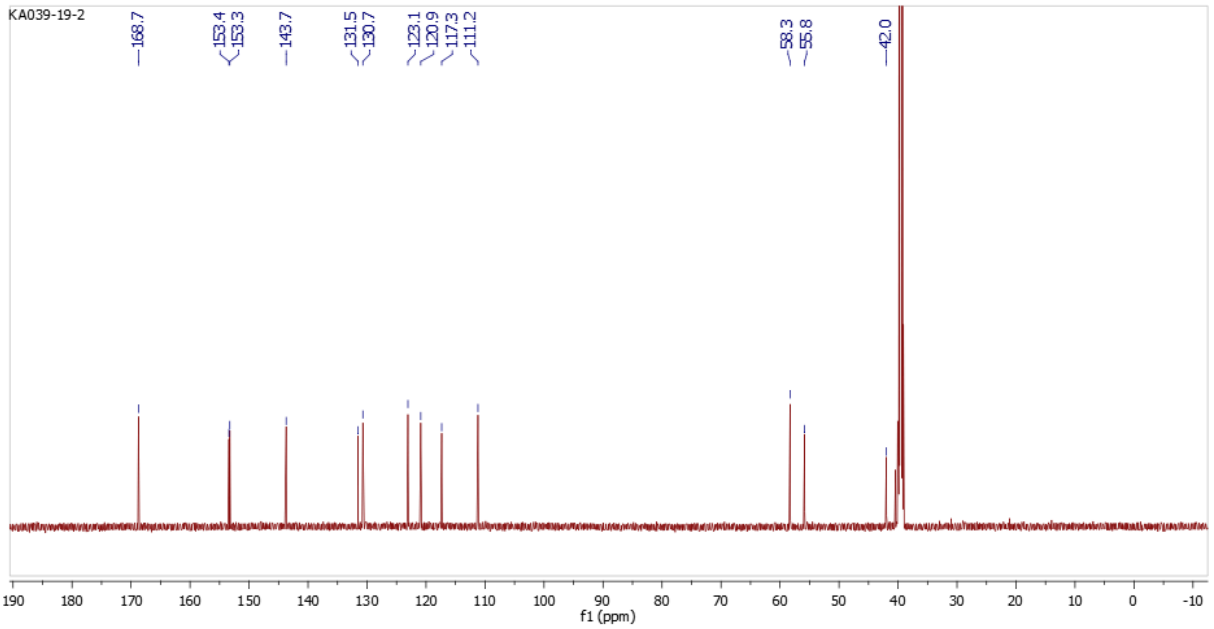

Figure 21. ^{13}C- NMR (150 MHz, DMSO-d_6) spectrum of compound **8**.

FT-IR (solid, cm^{-1}): 2605 (w), 2344 (w), 1731 (m), 1680 (m), 1601 (s), 1589 (s), 1504 (m), 1470 (m), 1401 (s), 1338 (s), 1276 (m), 1144 (m), 1118 (m), 1688 (w), 941 (m), 790 (m), 750 (s), 549 (m), 511 (m), 438 (s).

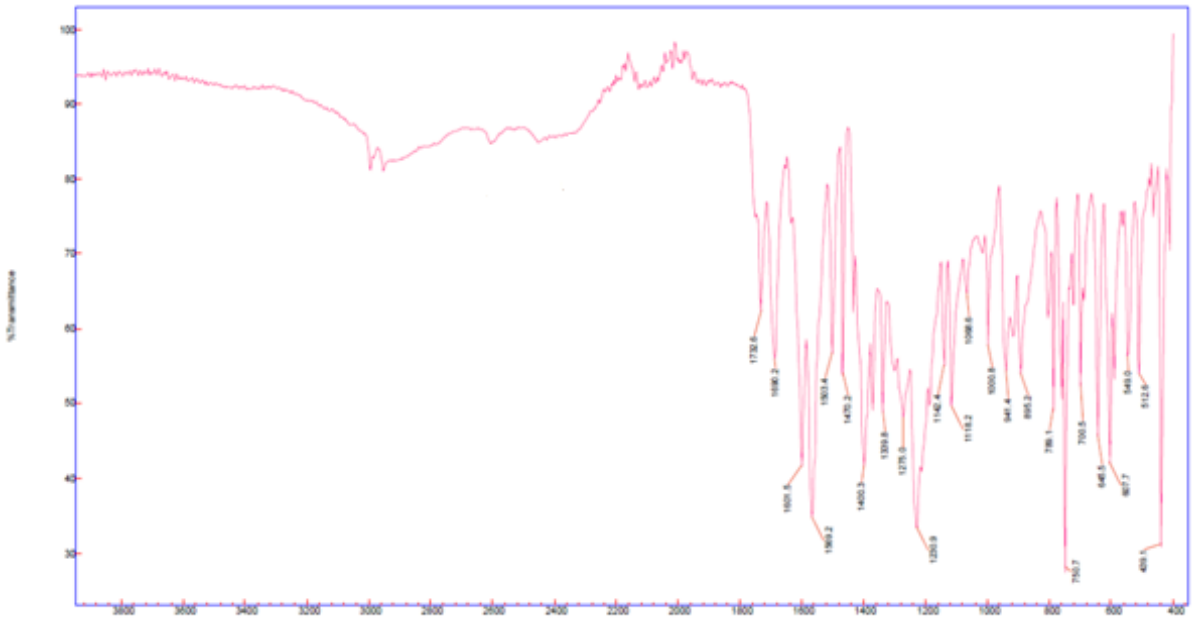

Figure 22. FT-IR (solid, cm^{-1}) spectrum of compound **8**.

MS (ESI m/z, negative ion mode): 287.0 (82 %) $[M-H]^-$, 243.0 (13 %) $[M-CO_2-H]^-$.

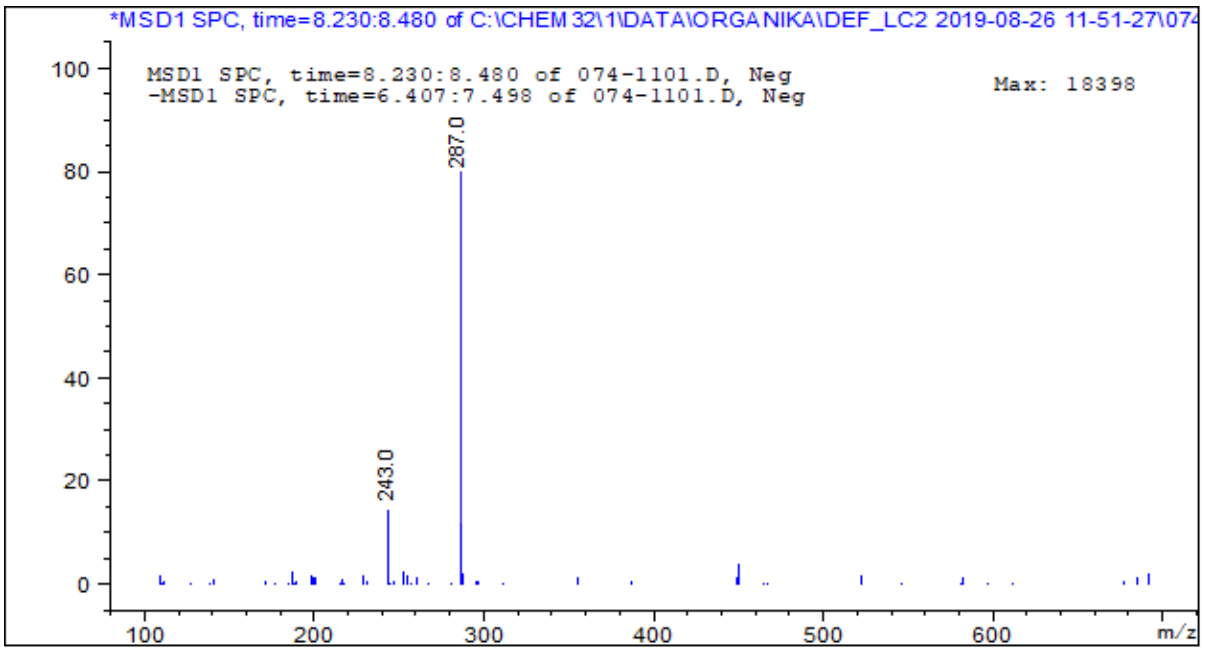

Figure 23. MS (ESI m/z, negative ion mode) spectrum of compound **8**.

Elemental analysis. Anal. Calc for $C_{13}H_{12}N_4O_4$ (288.26): C, 54.17; H, 4.20; N, 19.44; found: C, 54.53; H, 4.12; N, 19.35.

Ethyl 2-(2-(2-methoxyethyl)-3-oxo-2,3-dihydro-5*H*-[1,2,4]triazino[5,6-*b*]indol-5-yl)acetate (10**)**

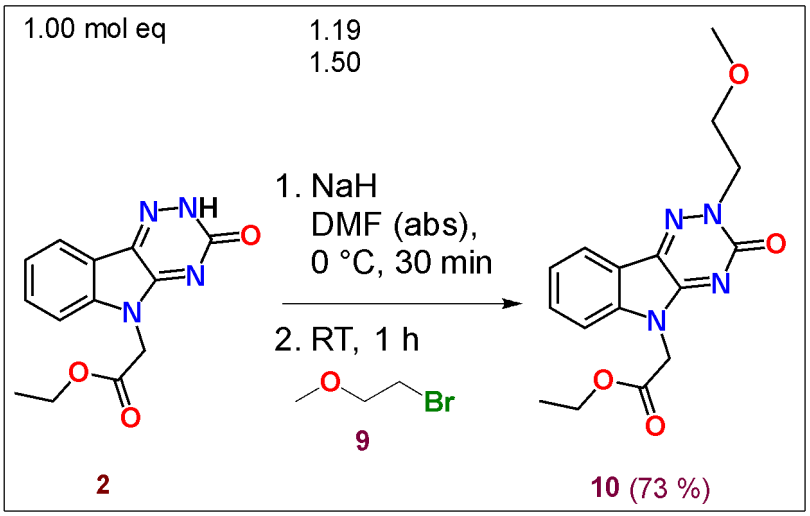

A solution of 100 mg (0.37 mmol, 1.00 mol eq) **2** in 1.0 mL of DMF (abs) was treated by 17.5 mg (0.44 mmol, 1.19 mol eq) of NaH. The reaction was stirred in an ice-bath within 30 min. Afterwards 52.5 µL (77.7 mg, 0.56 mmol, 1.51 mol eq) of 2-bromoethyl methyl ether (**9**) (d: 1.48 g/mL) was added and the mixture stirred at RT for 1 h. TLC analysis (SiO_2, Hex / EA, 1 / 5) confirmed conversion of **2** to a novel compound. Then, the mixture was extracted with EA (3 x 30 mL). Combined organic layer was washed with brine (5 x 30 mL) and dried by standing over Na_2SO_4. After filtration and RVE evaporation, product **10** was dried under high vacuum to yield 88.0 mg (0.27 mmol, 73 %) of yellow solid compound.

Novelty: Compound **10** was not yet described in the literature.
Melting point: 105.7 - 108.3 °C [EA]
NMR diagrams:

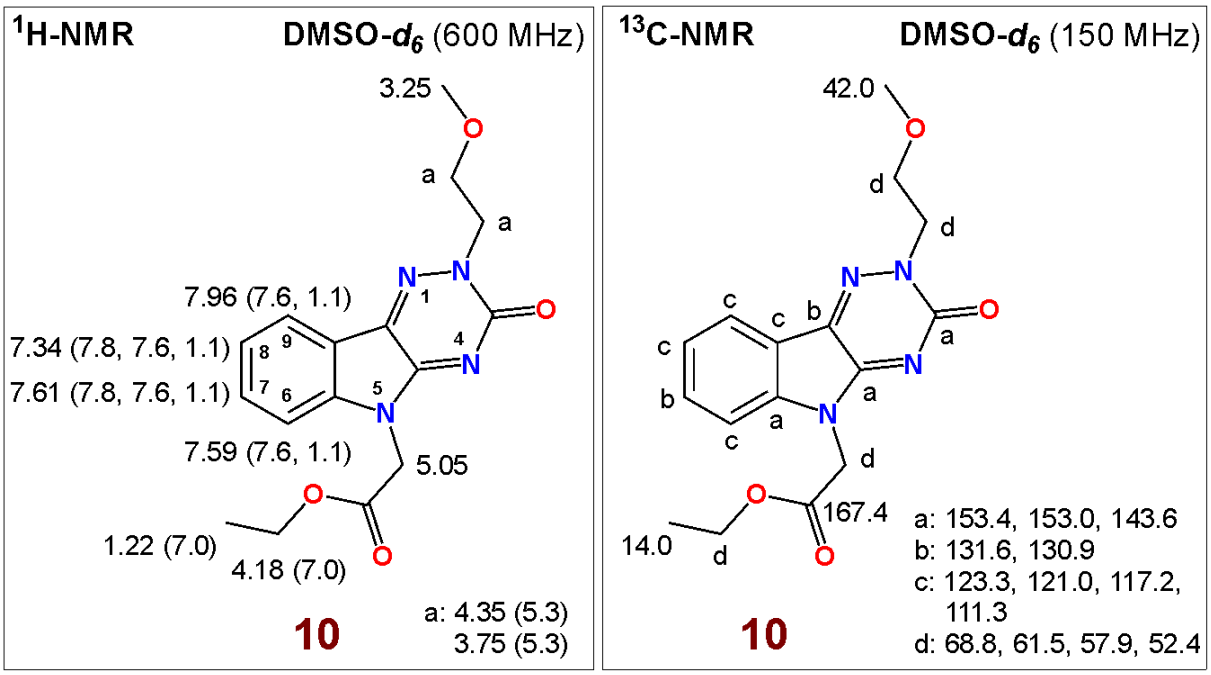

^{1}H-NMR: (600 MHz, DMSO-d_6): δ 7.96 (dd, 1H, J(8,9) = 7.6 Hz, J(7,9) = 1.1 Hz, H-C(9)), 7.61 (ddd, 1H, J(7,8) = 7.8 Hz, J(6,7) = 7.6 Hz, J(7,9) = 1.1 Hz, H-C(7)), 7.59 (dd, 1H, J(6,7) = 7.6 Hz, J(6,8) = 1.1 Hz, H-C(6)), 7.34 (ddd, 1H, J(7,8) = 7.8 Hz, J(8,9) = 7.6 Hz, J(6,8) = 1.1 Hz, H-C(8)), 5.05 (s, 2H, -C$\underline{H}_2$-N(5)), 4.35 (t, 2H, J(CH_2,CH_3) = 5.3 Hz, -N(2)$CH_2C\underline{H}_2OCH_3$ or -N(2)$C\underline{H}_2CH_2OCH_3$), 4.18 (q, 2H, J(CH_2,CH_3) = 7.0 Hz, -COOC$\underline{H}_2CH_3$), 3.75 (t, 2H, J(CH_2,CH_3) = 5.3 Hz, -N(2)$CH_2C\underline{H}_2OCH_3$ or -N(2)$C\underline{H}_2CH_2OCH_3$), 3.25 (s, 3H, -$CH_2OC\underline{H}_3$), 1.22 (t, 3H, J(CH_2,CH_3) = 7.0 Hz, -$COOCH_2C\underline{H}_3$).

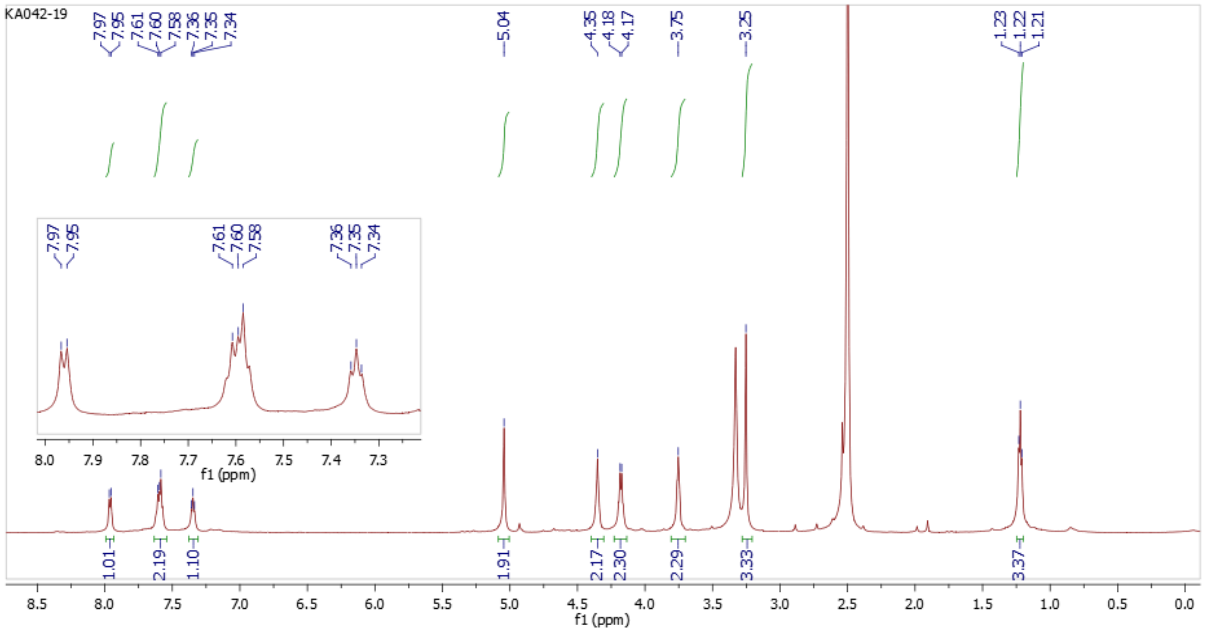

Figure 24. ^{1}H-NMR (600 MHz, DMSO-d_6) spectrum of compound **10**.

^{13}C-NMR: (150 MHz, DMSO-d_6): δ 167.4 (-$\underline{C}OOCH_2CH_3$), 153.4, 153.0, 143.6, 131.6, 130.9, 123.3, 121.0, 117.2, 111.3, 68.8, 61.5, 57.9, 52.4, 42.0,
14.0 (-$COOCH_2\underline{C}H_3$).

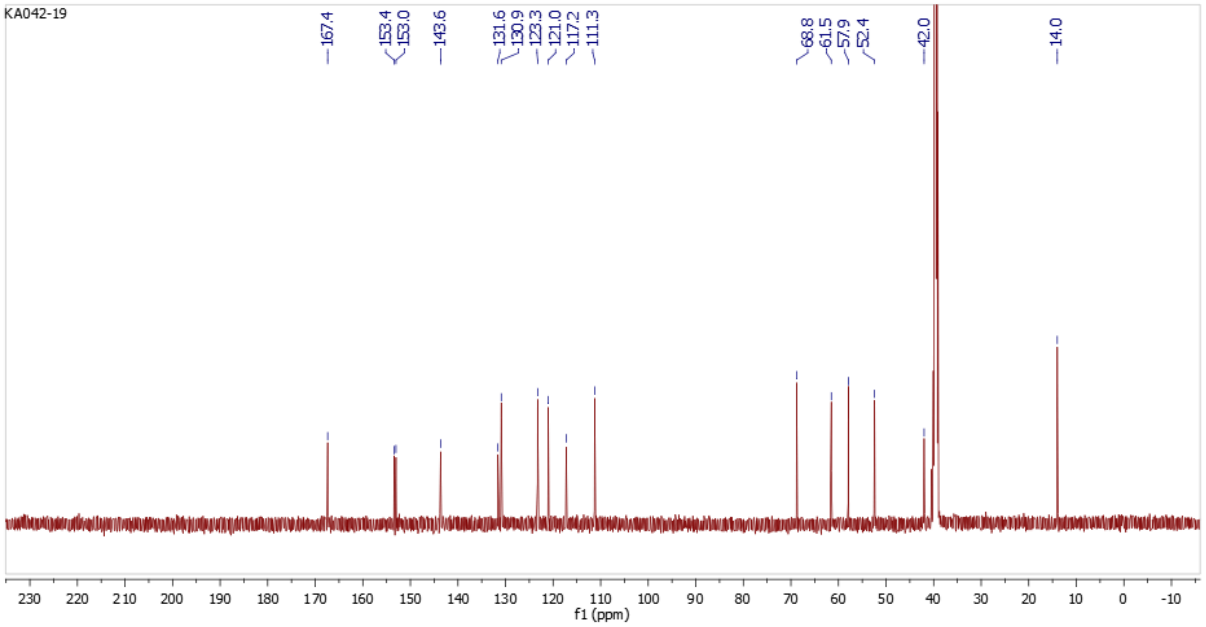

Figure 25. ^{13}C- NMR (150 MHz, DMSO-d_6) spectrum of compound **10**.

FT-IR (solid, cm^{-1}): 3050 (w), 2988 (w), 2932 (w), 1743 (s), 1671 (s), 1631 (s), 1604 (s), 1570 (s), 1495 (m), 1465 (m), 1422 (m), 1406 (m), 1325 (m), 1270 (m), 1150 (s), 1162 (s), 1066 (s), 1004 (s), 975 (m), 788 (s), 608 (s).

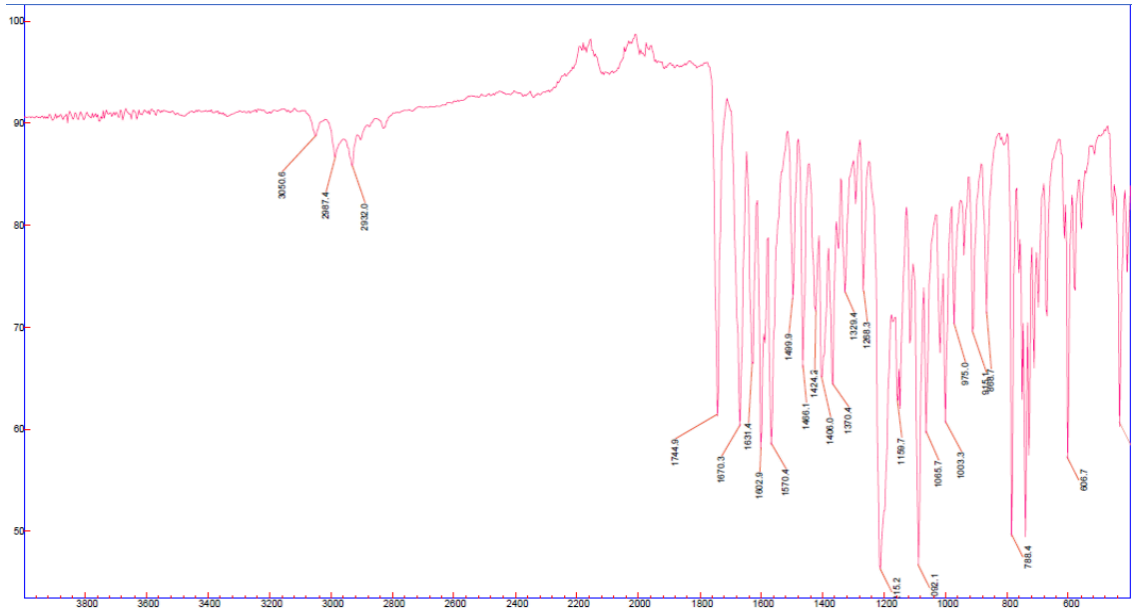

Figure 26. FT-IR (solid, cm^{-1}) spectrum of compound **10**.

MS (ESI m/z, positive ion mode): 331.0 $[M+H]^+$

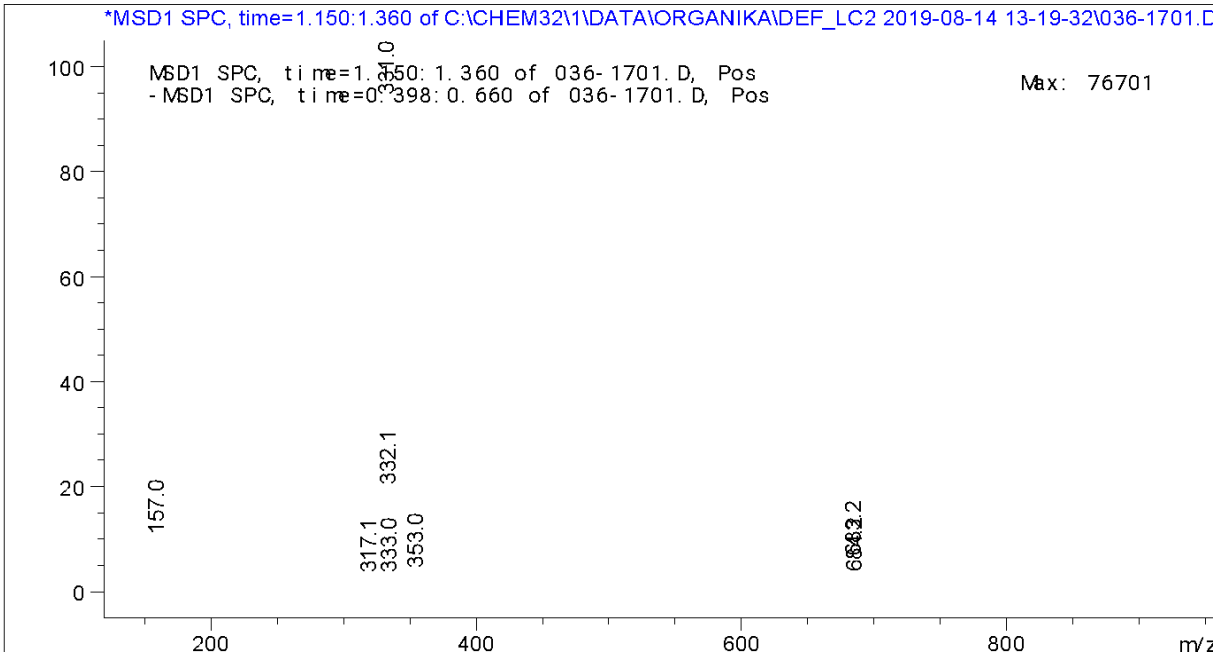

Figure 27. MS (ESI m/z, positive ion mode) spectrum of compound **10**.

Elemental analysis. Anal. Calc for $C_{16}H_{18}N_4O_4$ (330.34): C, 58.17; H, 5.49; N, 16.96 found: C, 58.23; H, 5.39; N, 16.75.

2-(2-(2-Methoxyethyl)-3-oxo-2,3-dihydro-5*H*-[1,2,4]triazino[5,6-*b*]indol-5-yl)acetic acid (11)

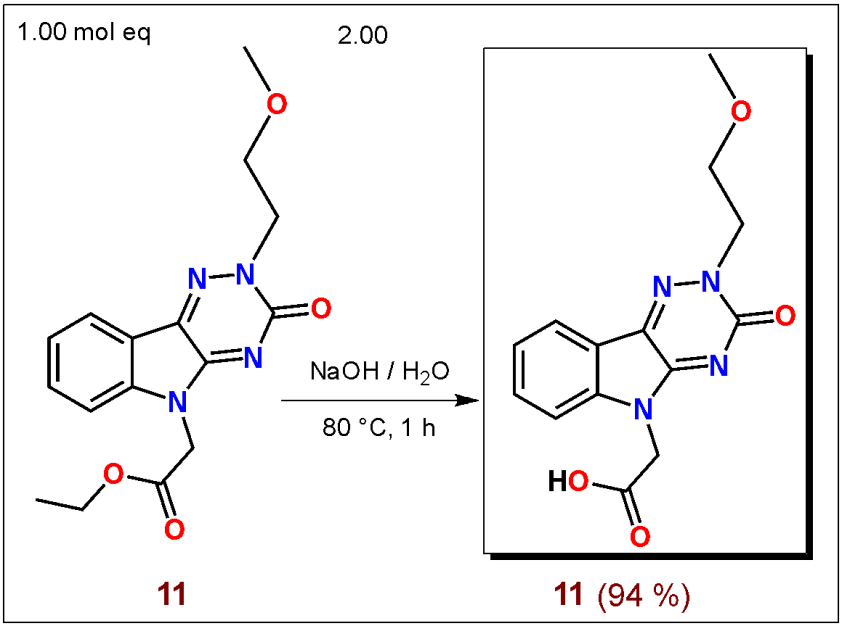

Ethyl ester **10** 60.0 mg (0.18 mmol, 1.00 mol eq) was dissolved in an aqueous solution of 14.5 mg (0.36 mmol, 2.00 mol eq) NaOH in 1.00 mL of H_2O. The reaction was stirred at 80 °C for 1 h. Complete conversion of **10** was confirmed by TLC analysis (SiO_2, MeOH / EA = 1 / 1). Afterwards the mixture was cooled down in an ice bath and acidified with 1 M HCl aq solution to pH 2. Precipitated product **11** was filtered off and purified by crystallisation from a mixture of H_2O / HCl. Yellow crystals were isolated by filtration and dried under high vacuum to yield 50.1 mg (0.17 mmol, 94 %) of acid **11**.

Novelty: Compound **11** was not yet described in the literature.

Melting point: 230.8 - 235.6 °C [H_2O / HCl]

NMR diagrams:

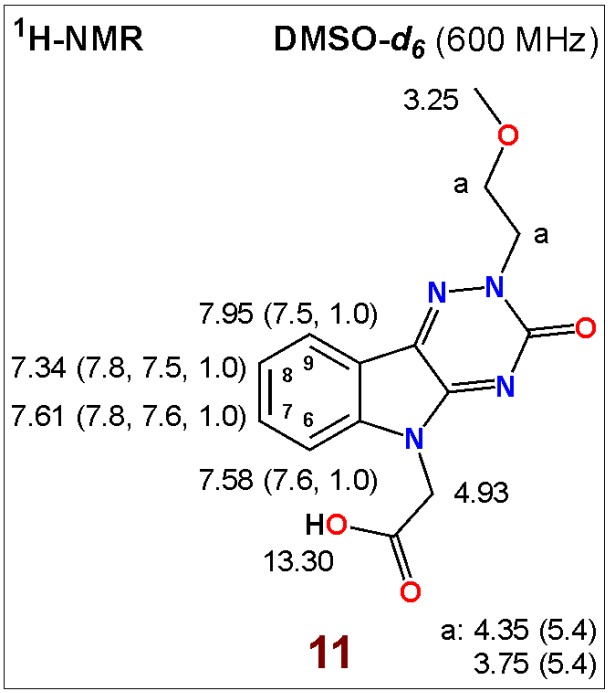

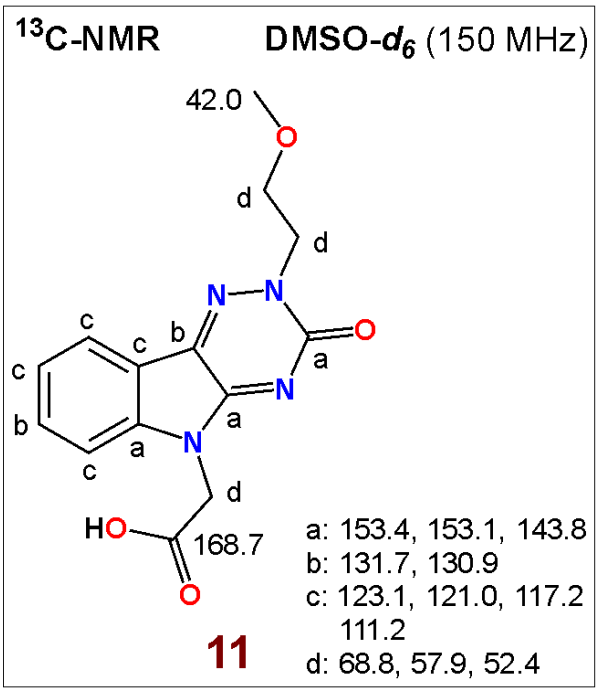

^{1}H-NMR: (600 MHz, DMSO-d_6): δ **13.30** (br s, 1H, -COOH), **7.95** (dd, 1H, J(8,9) = 7.5 Hz, J(7,9) = 1.0 Hz, H-C(9)), **7.61** (ddd, 1H, J(7,8) = 7.8 Hz, J(6,7) = 7.6 Hz, J(7,9) = 1.0 Hz, H-C(7)), **7.58** (dd,

1H, *J*(6,7) = 7.6 Hz, *J*(6,8) = 1.0 Hz, H-C(6)), 7.34 (ddd, 1H, *J*(7,8) = 7.8 Hz, *J*(8,9) = 7.5 Hz, *J*(6,8) = 1.0 Hz, H-C(8)), 4.93 (s, 2H, -C$\underline{H}_2$-COOH), 4.35 and 3.75 (2 x t, 2 x 2H, 2 x *J*(CH_2,CH_3) = 5.4 Hz, -N(2)$CH_2C\underline{H}_2OCH_3$) and N(2)$C\underline{H}_2CH_2OCH_3$), 3.25 (s, 3H, -$OCH_3$).

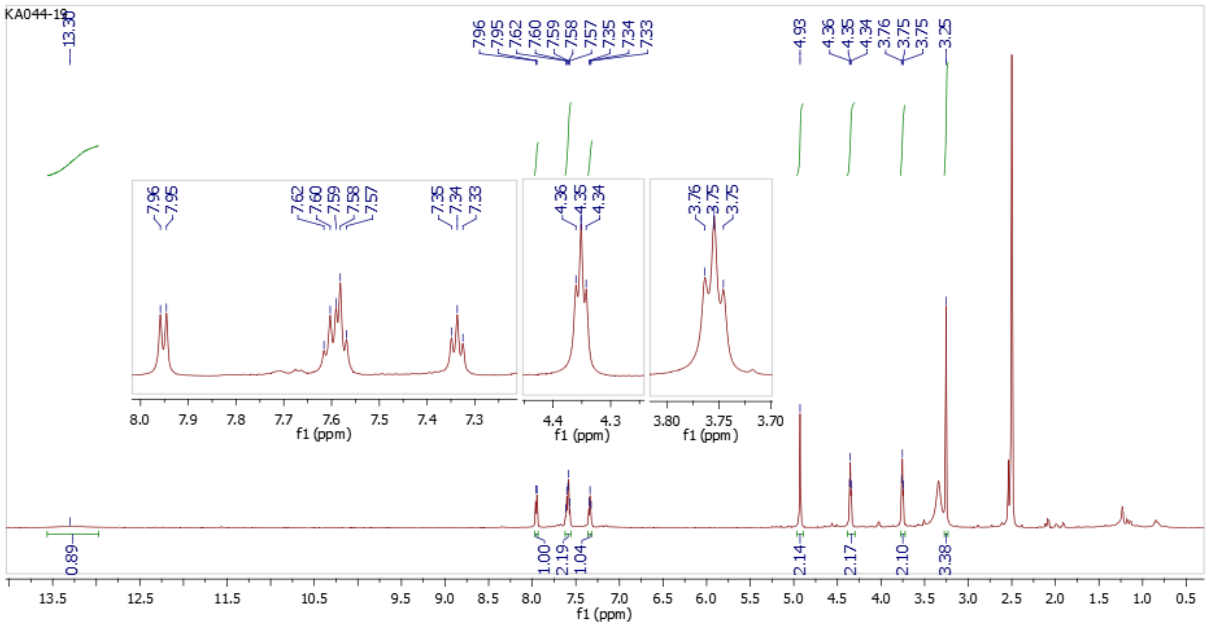

Figure 28. [1]H-NMR (600 MHz, DMSO-d_6) spectrum of compound **11**.

[13]C-NMR: (150 MHz, DMSO-d_6): δ 168.7 (-COOH), 153.4, 153.1, 143.8, 131.7, 130.9, 123.1, 121.0, 117.2, 111.2, 68.8, 57.9, 52.4, 42.0.

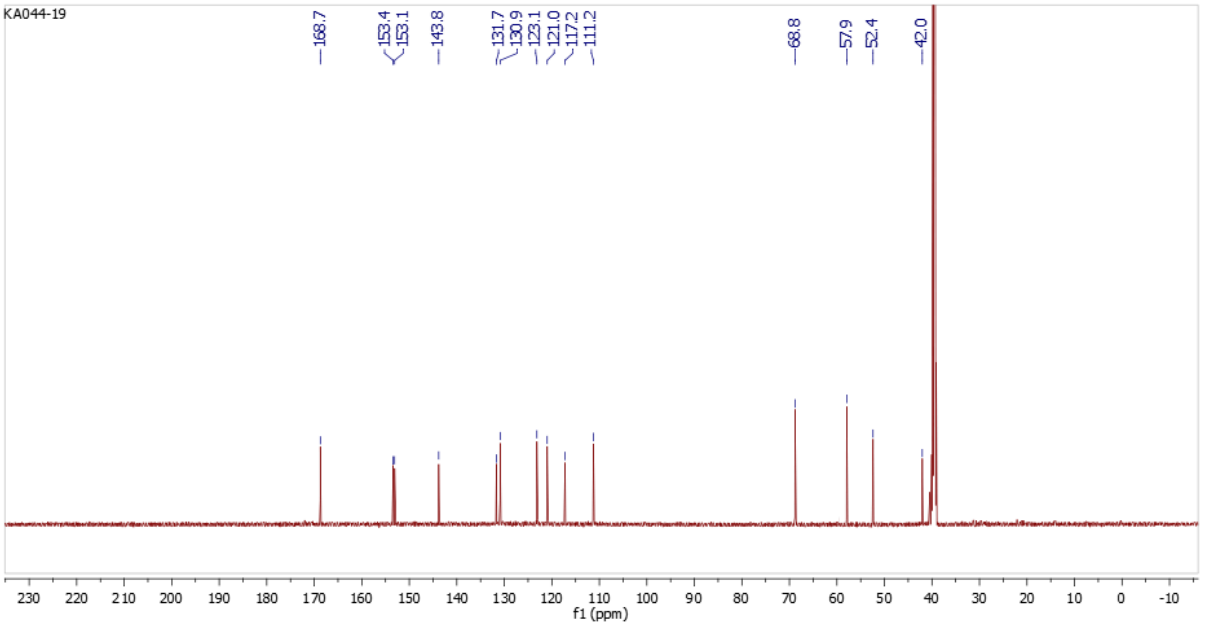

Figure 29. [13]C- NMR (150 MHz, DMSO-d_6) spectrum of compound **11**.

FT-IR (solid, cm^{-1}): 3244 (w), 2918 (w), 1741 (s), 1607 (s), 1576 (s), 1464 (m), 1411 (m), 1308 (m), 1266 (m), 1218 (s), 1166 (s), 1088 (s), 1006 (s), 914 (s), 891 (m), 757 (s), 747 (s), 670 (m).

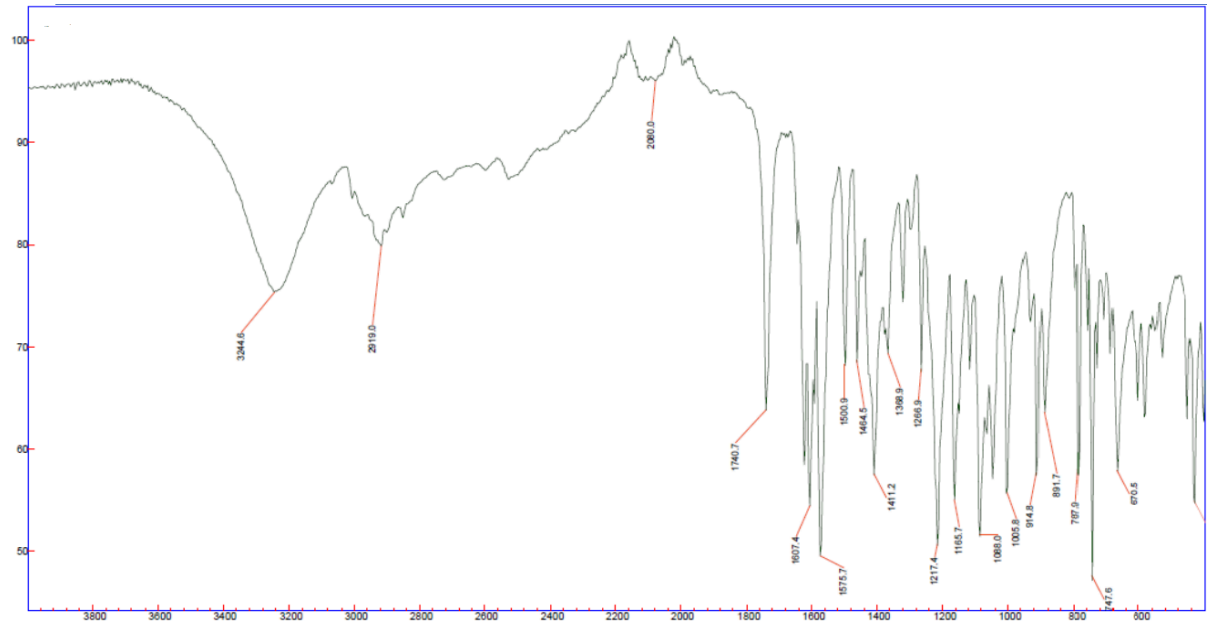

Figure 30. FT-IR (solid, cm^{-1}) spectrum of compound **11**.

MS (ESI m/z, negative ion mode): 301.1 (100 %) $[M-H]^-$, 257.1 (47 %) $[M-CO_2-H]^-$.

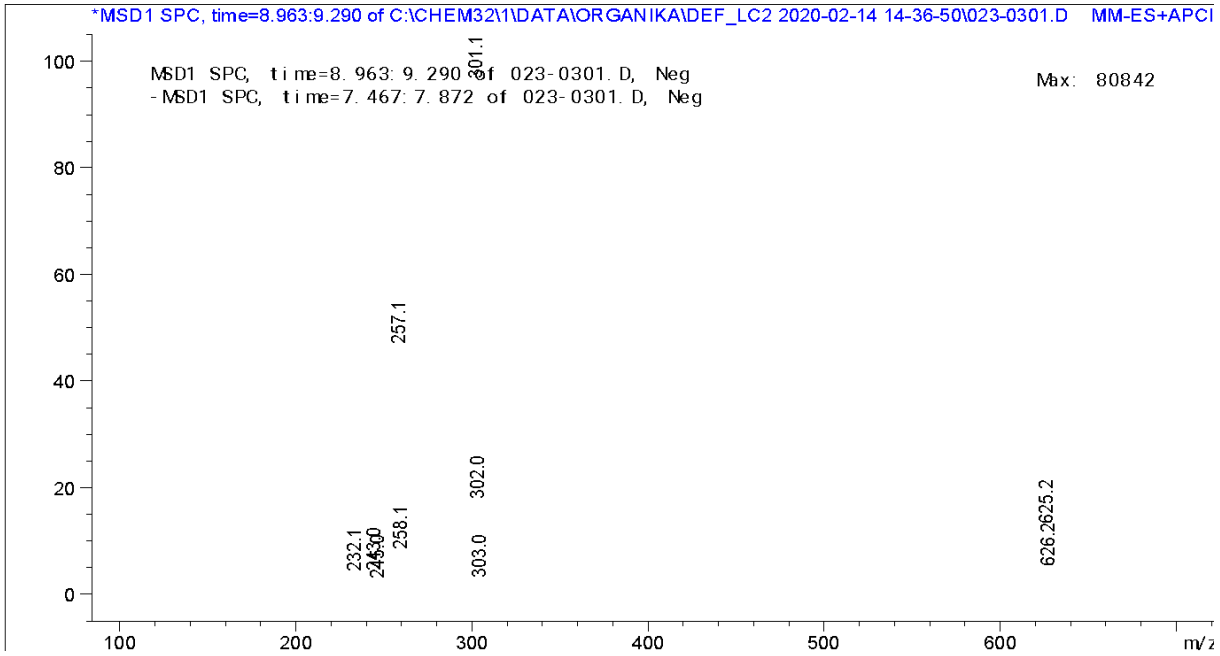

Figure 31. MS (ESI m/z, negative ion mode) spectrum of compound **11**.

Elemental analysis. Anal. Calc for $C_{14}H_{14}N_4O_4$ (302.29): C, 55.63; H, 4.67; N, 18.53 found: C, 55.53; H, 4.49; N, 18.79.

Ethyl 3-(5-(2-ethoxy-2-oxoethyl)-3-oxo-3,5-dihydro-2*H*-[1,2,4]triazino[5,6-*b*]indol-2-yl)propanoate (13)

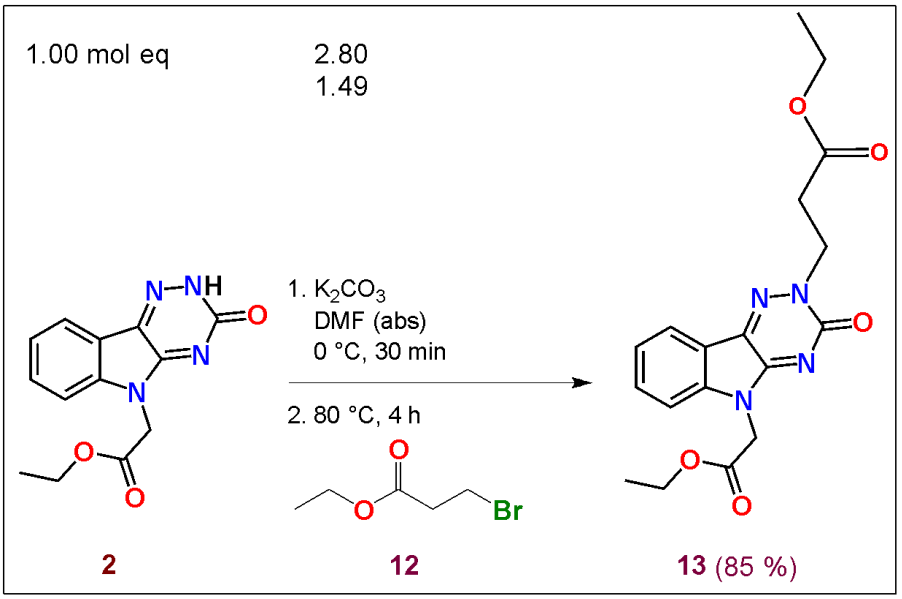

A solution of 150 mg (0.55 mmol, 1.00 mol eq) **2** in 1.5 mL of DMF (abs) was treated by 213.2 mg (1.54 mmol, 2.80 mol eq) of K_2CO_3. The reaction was stirred in an ice bath within 30 min. Afterwards 105.7 µL (149.0 mg, 0.82 mmol, 1.49 mol eq) of ethyl 3-bromopropanoate (**12**) (d: 1.41 g/mL) was added and the reaction stirred at 80 °C for 4 h. TLC analysis (SiO_2, Hex / EA, 1 / 5) confirmed conversion of **2** to a novel compound. Then, the mixture was extracted with EA (3 x 100 mL). Combined organic layer was washed with brine (5 x 100 mL) and dried by standing over Na_2SO_4. After filtration and RVE evaporation, product **13** was dried under high vacuum to yield 174.1 mg (0.47 mmol, 85 %).

Novelty: Compound **13** was not yet described in the literature.
Melting point: 121.7 - 125.3 °C [EA]
NMR diagrams:

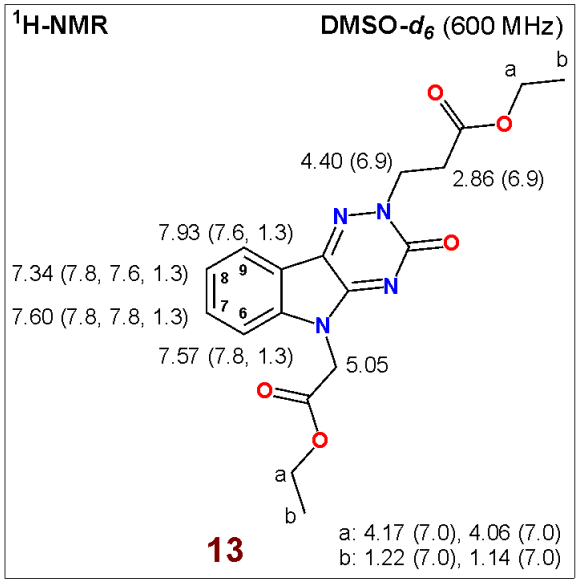

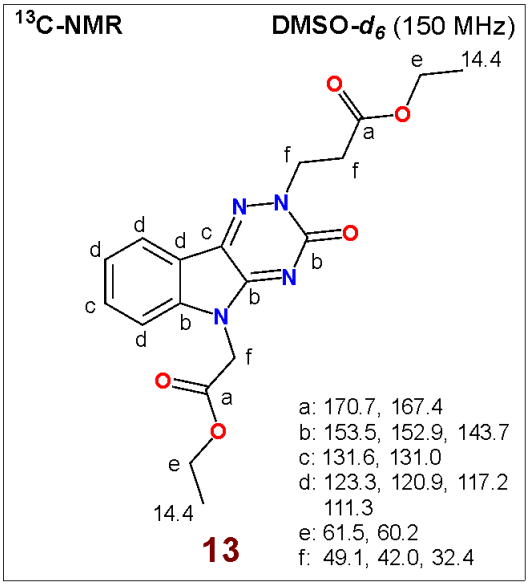

^{1}H-NMR: (600 MHz, DMSO-d_6): δ 7.93 (dd, 1H, J(8,9) = 7.6 Hz, J(7,9) = 1.3 Hz, H-C(9)), 7.60 (ddd, 1H, J(7,8) = 7.8 Hz, J(6,7) = 7.8 Hz, J(7,9) = 1.3 Hz, H-C(7)), 7.57 (dd, 1H, J(6,7) = 7.8 Hz, J(6,8) = 1.3 Hz, H-C(6)), 7.34 (ddd, 1H, J(7,8) = 7.8 Hz, J(8,9) = 7.6 Hz, J(6,8) = 1.3 Hz, H-C(8)), 5.05 (s, 2H, -N(5)CH_2), 4.40 (t, 2H, J(CH_2,CH_2) = 6.9 Hz, -N(2)C<u>H</u>$_2$$CH_2$-), 4.17 and 4.06 (2 x q, 2 x 2H, 2 x J(CH_2,CH_3) = 7.0 Hz, 2 x -COOC<u>H</u>$_2$$CH_3$), 2.86 (t, 2H, J(CH_2,CH_2) = 6.9 Hz, -N(2)CH_2C<u>H</u>$_2$-), 1.22 and 1.14 (2 x t, 2 x 3H, 2 x J(CH_2,CH_3) = 7.0 Hz, 2 x -COOCH_2C<u>H</u>$_3$).

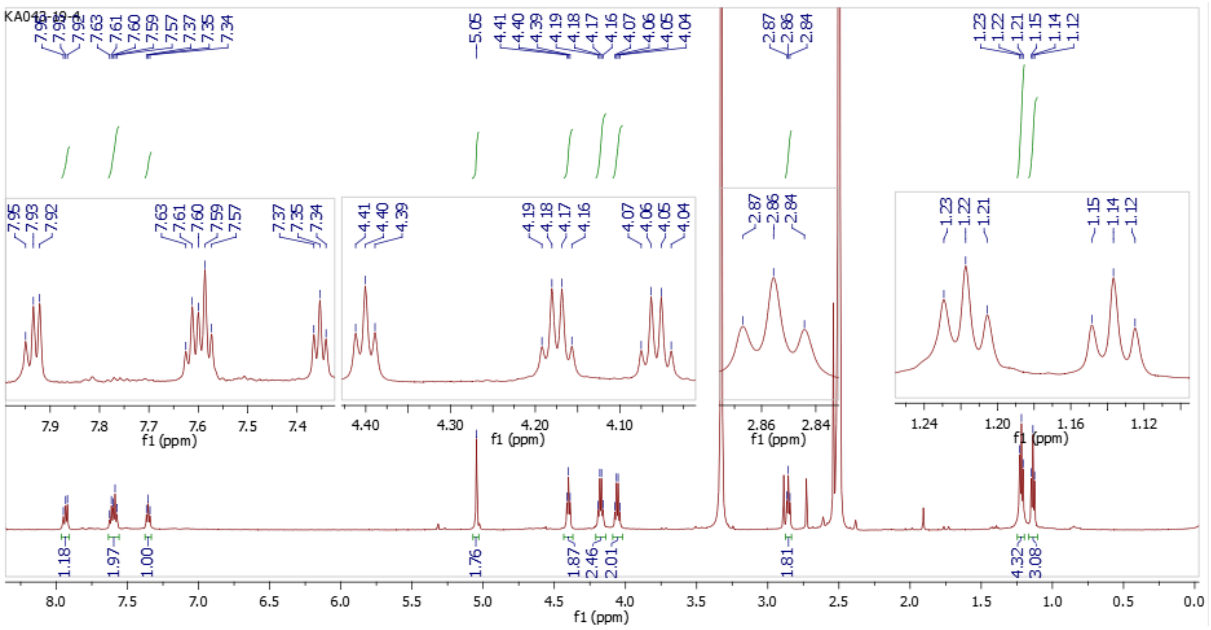

Figure 32. ^{1}H-NMR (600 MHz, DMSO-d_6) spectrum of compound **13**.

^{13}C-NMR: (150 MHz, DMSO-d_6): δ 170.7, 167.4, 153.5, 152.9, 143.7, 131.6, 131.0, 123.3, 120.9, 117.2, 111.3, 61.5, 60.2, 49.1, 42.0, 32.4, 2 x 14.4 (2 x -$COOCH_2\underline{C}H_3$).

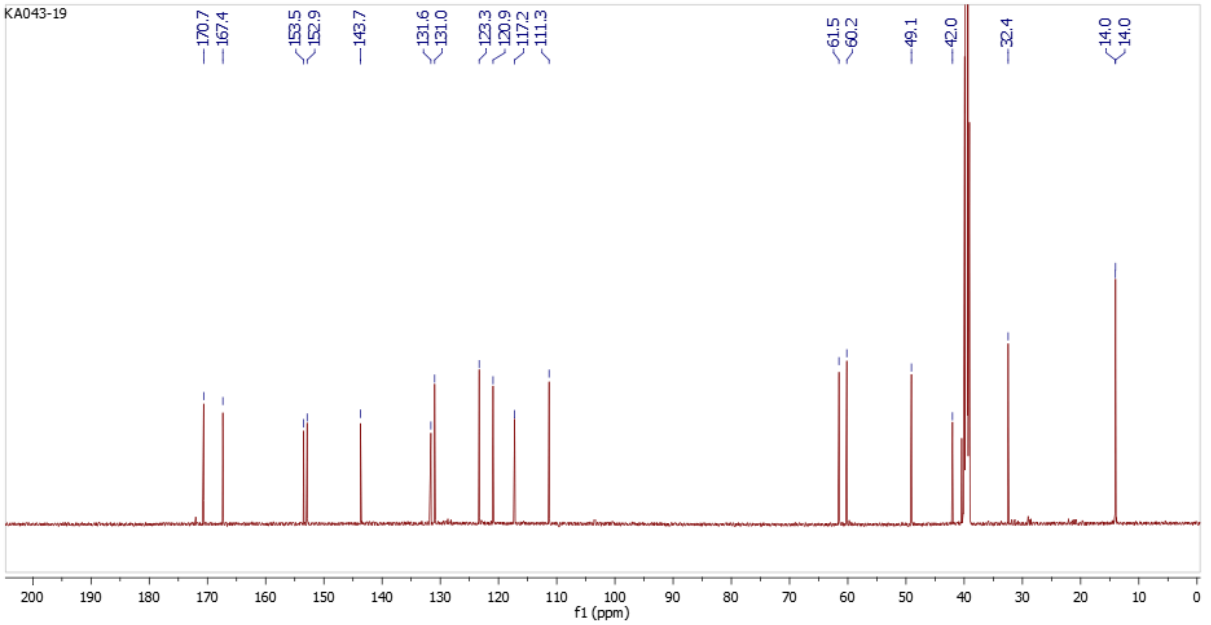

Figure 33. ^{13}C- NMR (150 MHz, DMSO-d_6) spectrum of compound **13**.

FT-IR (solid, cm^{-1}): 2989 (w), 2931 (w), 1736 (s), 1780 (s), 1679 (s), 1630 (s), 1570 (m), 1497 (w), 1423 (s), 1410 (s), 1372 (m), 1330 (s), 1306 (w), 1273 (m), 1213 (s), 1181 (s), 1099 (s), 1060 (m), 1025 (m), 1104 (s), 980 (m), 930 (m), 872 (w), 783 (s), 752 (s), 730 (s), 702 (s), 669 (w), 581 (m), 548 (w), 487 (w), 432 (m), 454 (m).

Figure 34. FT-IR (solid, cm^{-1}) spectrum of compound **13**.

MS (APCI m/z, positive ion mode): 373.1 (100 %) $[M+H]^+$, 327.0 $[M\text{-}OEt]^+$ (70 %), 273.0 $[M\text{-}CH_2CH_2COOEt+2H]^+$ (85 %).

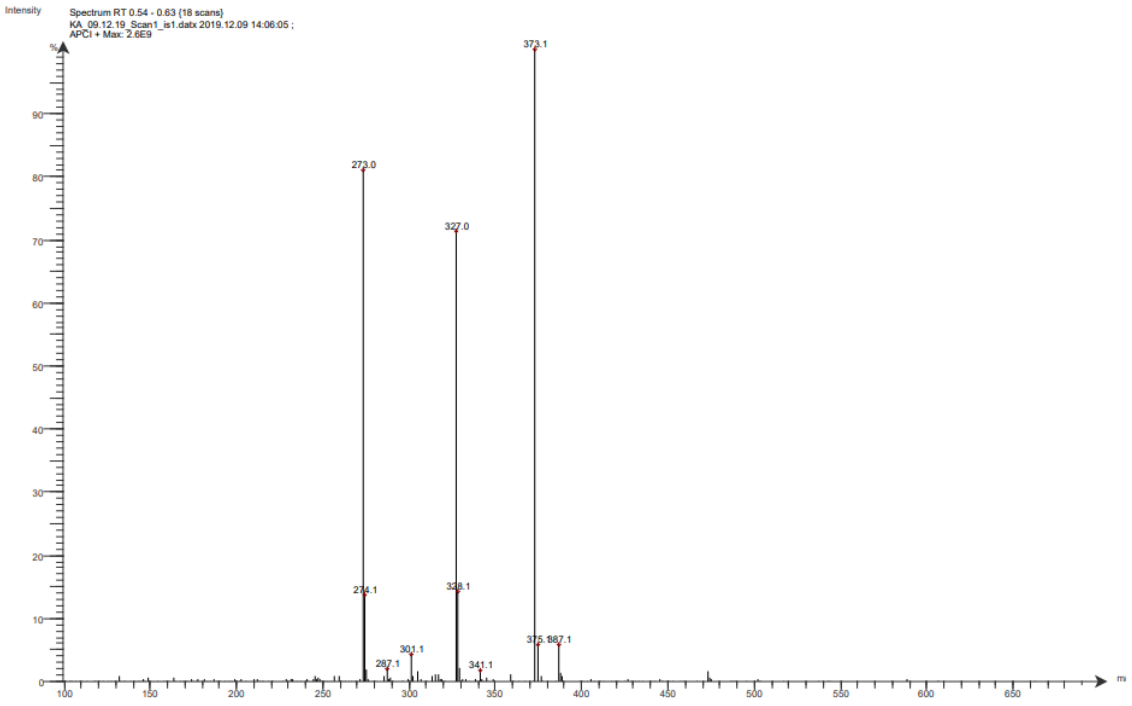

Figure 35. MS (APCI m/z, positive ion mode) spectrum of compound **13**.

Elemental analysis. Anal. Calc for $C_{18}H_{20}N_4O_5$ (372.38): C, 58.06; H, 5.41; N, 15.05; found: C, 57.95; H, 5.49; N, 14.79.

3-(5-(Carboxymethyl)-3-oxo-3,5-dihydro-2*H*-[1,2,4]triazino[5,6-*b*]indol-2-yl)propanoic acid (13)

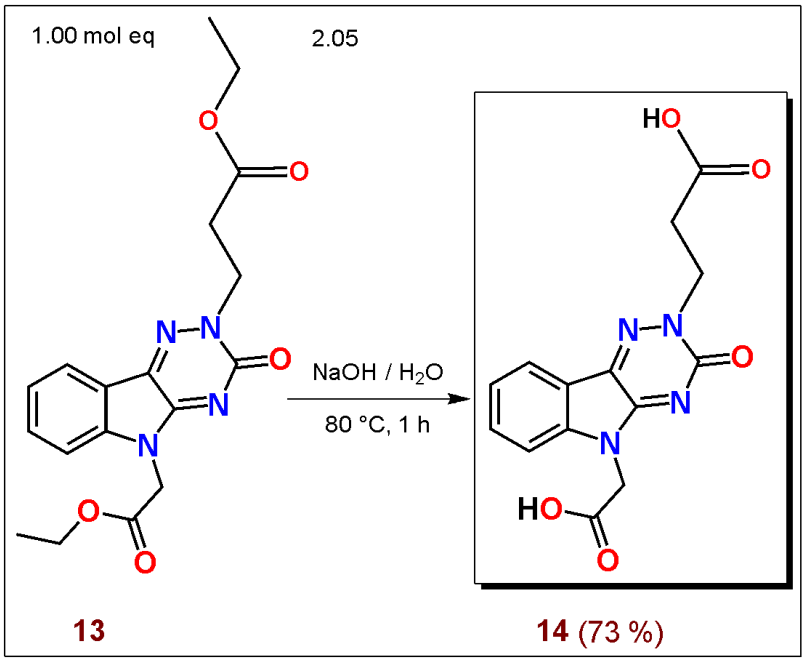

Ethyl ester **13** 83.0 mg (0.22 mmol, 1.00 mol eq) was dissolved in aqueous solution of 17.8 mg (0.45 mmol, 2.05 mol eq) NaOH in 1.00 mL of H_2O.The reaction mixture was stirred at 80 °C for 1 h. Complete conversion of **13** was confirmed by TLC analysis (SiO_2, MeOH / EA = 1 / 1). Afterwards the reaction was cooled down in an ice bath and acidified by 1 M HCl aq solution to pH 2. Precipitated product **14** was filtered off and purified by crystallisation from a mixture of H_2O / HCl. Yellow crystals were isolated by filtration and dried under high vacuum to yield 50.1 mg (0.16 mmol, 73 %) of compound **14**.

Novelty: Compound **14** was not yet described in the literature.

Melting point: 273.0 - 277.4 °C [H_2O / HCl]

NMR diagrams:

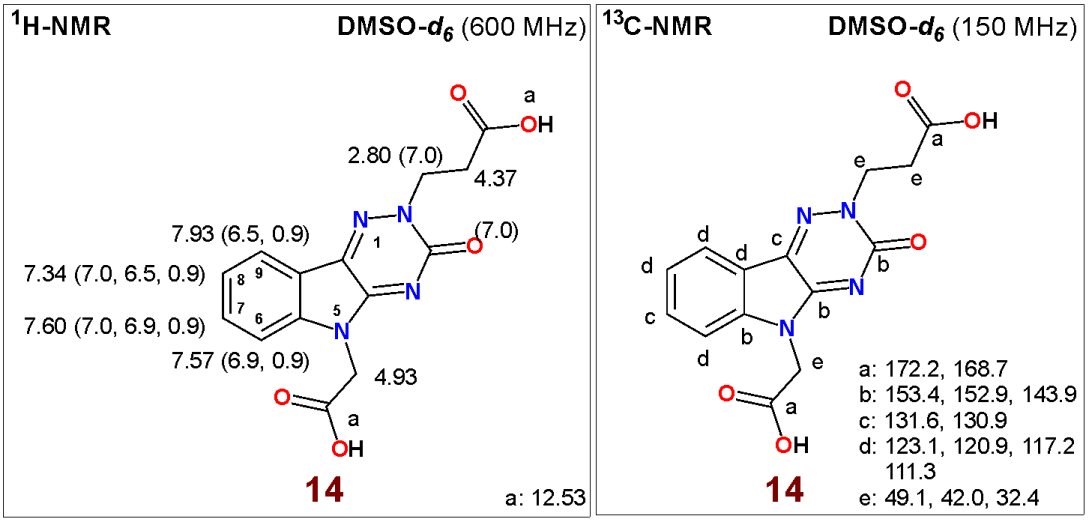

^{1}H-NMR: (600 MHz, DMSO-d_6): δ 12.53 (2 x br s, 2 x 1H, 2 x -COOH), 7.93 (d, 1H, J(8,9) = 6.5 Hz, J(7,9) = 0.9 Hz, H-C(9)); 7.60 (dd, 1H, J(7,8) = 7.0 Hz, J(6,7) = 6.9 Hz, J(7,9) = 0.9 Hz, H-C(7)); 7.57 (d, 1H, J(6,7) = 6.9 Hz, J(6,8) = 0.9 Hz, H-C(6)); 7.34 (dd, 1H, J(7,8) = 7.0 Hz, J(8,9) = 6.5 Hz, J(6,8) = 0.9 Hz, H-C(8)); 4.93 (s, 2H, -N(5)CH_2COOH), 4.37 (t, 2H, J(CH_2,CH_2) = 7.0 Hz, -N(2)CH_2CH_2COOH); 2.80 (t, 2H, J(CH_2,CH_2) = 7.0 Hz, -N(2)C$H_2$$CH_2$COOH).

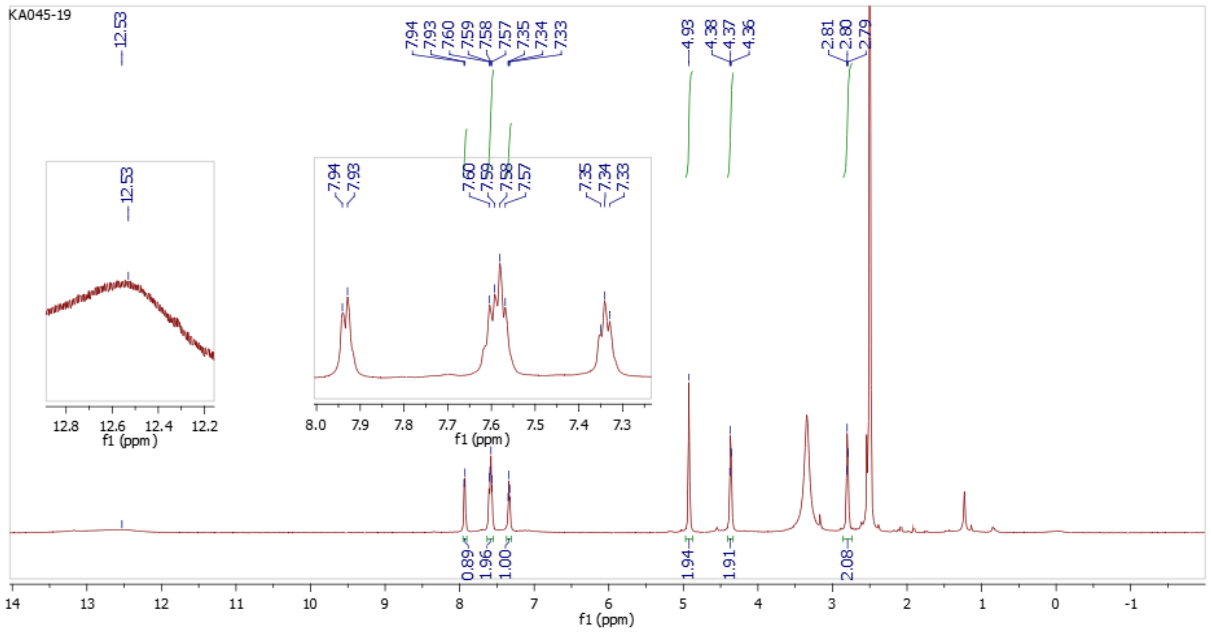

Figure 36. [1]H-NMR (600 MHz, DMSO-d_6) spectrum of compound **14**.

[13]C-NMR: (150 MHz, DMSO-d_6): δ 172.2, 168.7, 153.4, 152.9, 143.9, 131.6, 130.9, 123.1, 120.9, 117.2, 111.3, 49.1, 42.0, 32.4.

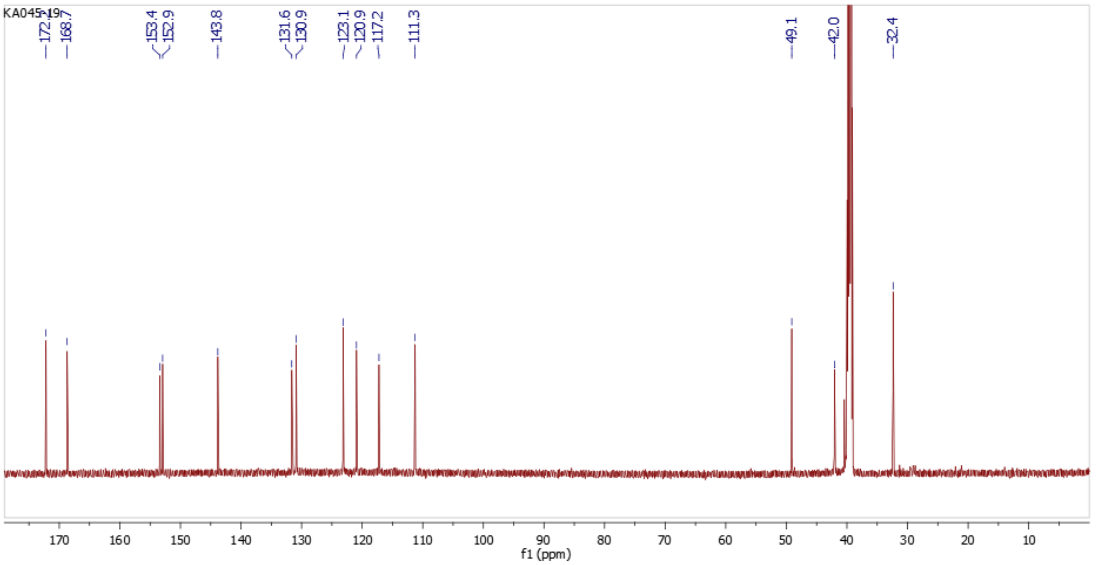

Figure 37. [13]C- NMR (150 MHz, DMSO-d_6) spectrum of compound **14**.

FT-IR (solid, cm^{-1}): 2924 (m), 2716 (w), 2598 (w), 2524 (w),1724 (s), 1641 (m), 1596 (m), 1596 (m), 1562 (m), 1502 (m), 1489 (m), 1406 (m), 1373 (s), 1324 (m), 1206 (s), 1134 (m), 1012 (m), 909 (m), 787 (s), 751 (s), 689 (w), 661 (w), 599 (w), 490 (w), 434 (w) cm^{-1}.

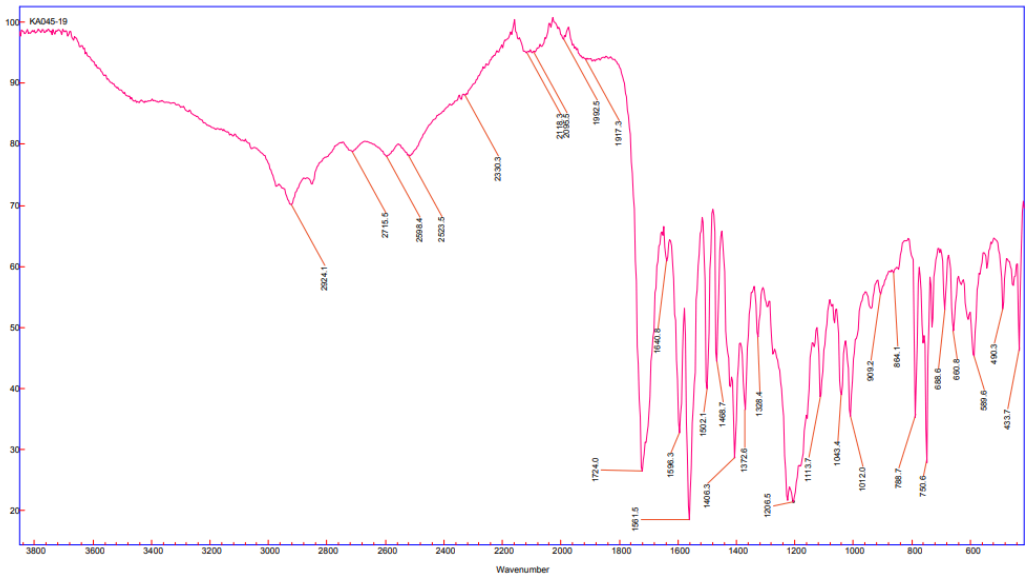

Figure 38. FT-IR (solid, cm^{-1}) spectrum of compound **14**.

MS (ESI m/z, positive ion mode): 317.1 $[M+H]^+$ (100 %).

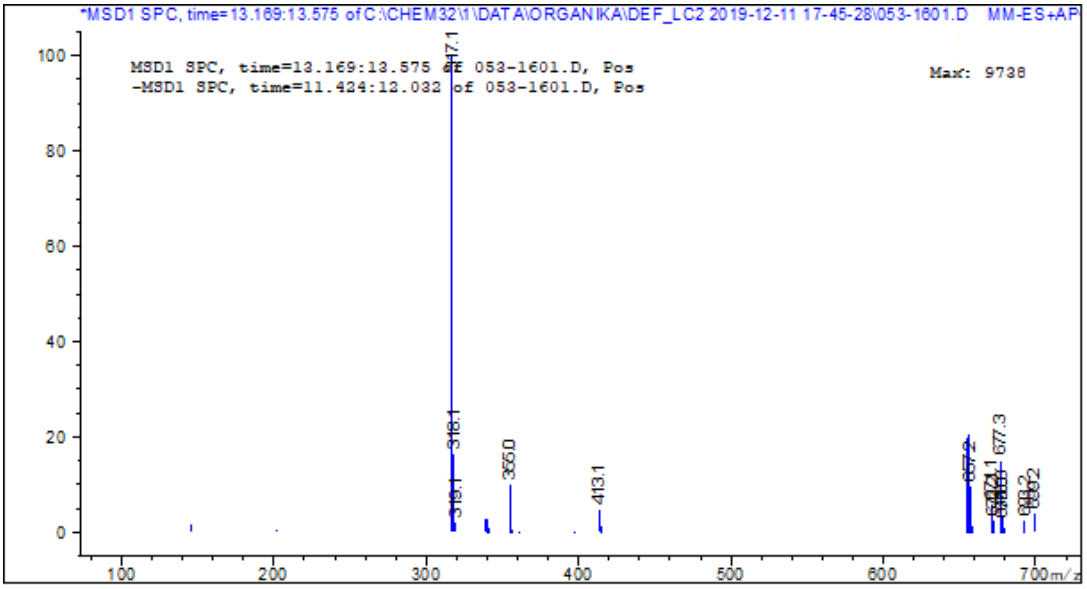

Figure 39. MS (ESI m/z, positive ion mode) spectrum of compound **14**.

Elemental analysis. Anal. Calc for $C_{14}H_{12}N_4O_5$ (316.27): C, 53.17; H, 3.82; N, 17.72; found: C, 53.05; H, 3.69; N, 17.59.

3. Drug Design

In our previous study (Kovacikova et al. *Molecules* 2021 in Fig. 7) compounds OTI and CMTI have similar binding poses. Proceeding from the X-ray structure of CMTI in ALR2 (PDB: 4QX4), we found possible enhancing of interaction energy in the *N(2)*-substitution (Fig. 40 - position of CMTI and its related interaction surface in ALR2). Moreover, the interaction surface preferred the substituents with a lipophilic linker and hydrophilic end interacting mainly with the residue of Ser302.

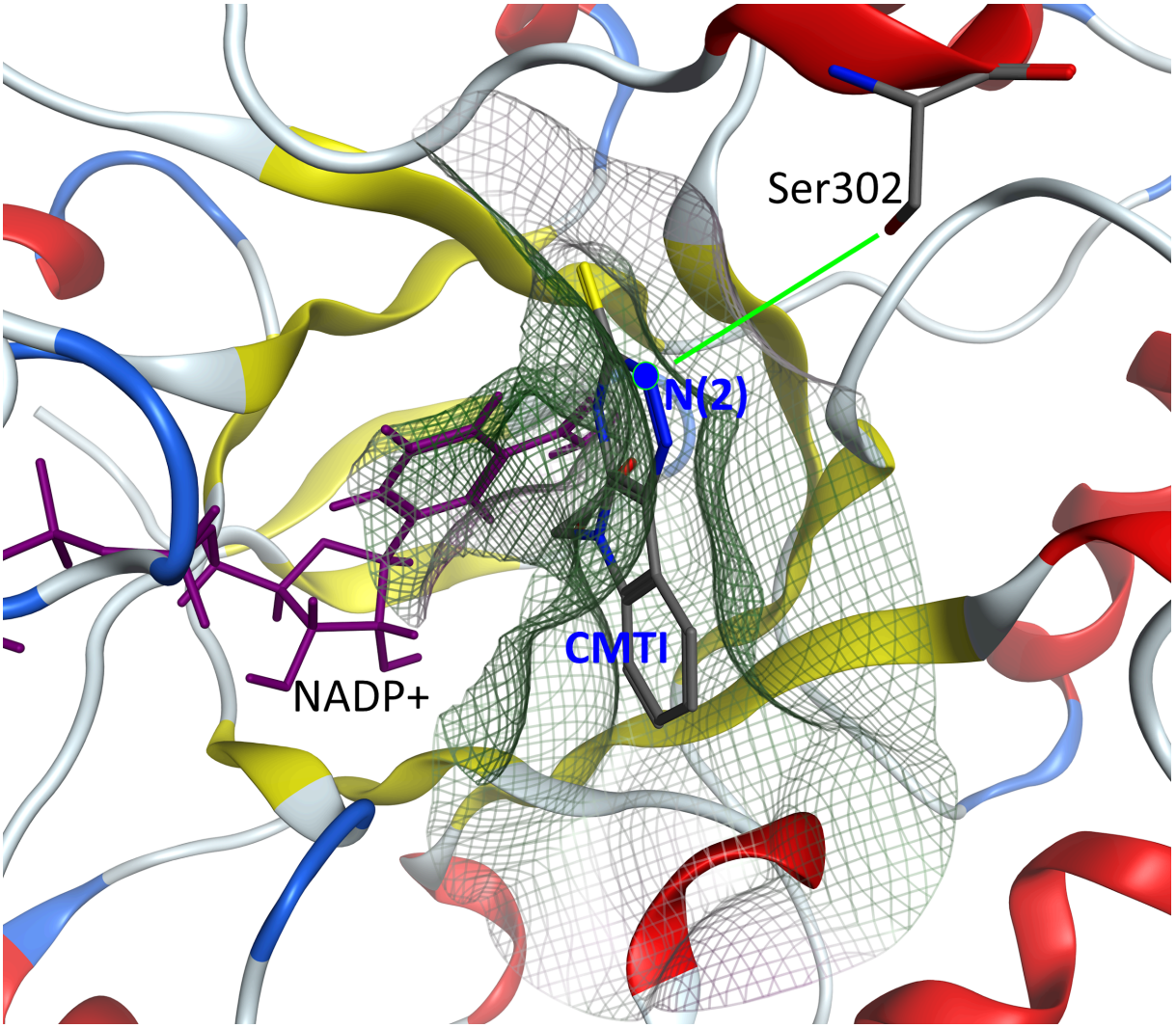

Figure 40. Position of **CMTI** and its related interaction surface in **AKR1B1** (X-ray structure with PDB code **4QX4**). The surface is colored according to lipophilic properties from the lipophilic (green) to the hydrophilic (violet) region. Visualized by program MOE[1].

This study involves the development of N(2)-substituted OTI derivatives **5**, **8**, **11**, and **14** to investigate a unoccupied specific pocket in aldose reductase (Hlavac et al. *Bioorg Med Chem* 2021). These compounds have been proposed by molecular modeling, binding predictions by docking, synthesis and biological screening. For docking a conformer of AKR1B1 (a human aldose reductase) was taken from a complex of the enzyme and CMTI (PDB: 4QX4) due to the ligand similarity. The aim was to get possible additional intermolecular interactions, e.g. hydrogen bonds from N(2)-substituted OTIs possessing an aliphatic chain with C=O, -OH, -OMe or -COOH groups. Additional hydrogen bonding of our new ligands were expected to form with -OH and -NH- groups of Ser302 and Leu301 from AKR1B1 as depicted on Fig. 41. From interaction analysis, it is obvious that the most key binding group in each of OTI inhibitors is a carboxylate that can form several ionic and hydrogen bonds. Searching of OTI derivatives can be useful to better understand the binding of OTI ligands inside the aldose reductase enzyme and selectivity of OTI ligands toward aldehyde reductase anti-target e.g. AKR1A1.

[1] Molecular Operating Environment (MOE), 2022.02 Chemical Computing Group ULC, 910-1010 Sherbrooke St. W., Montreal, QC H3A 2R7, Canada, 2024.

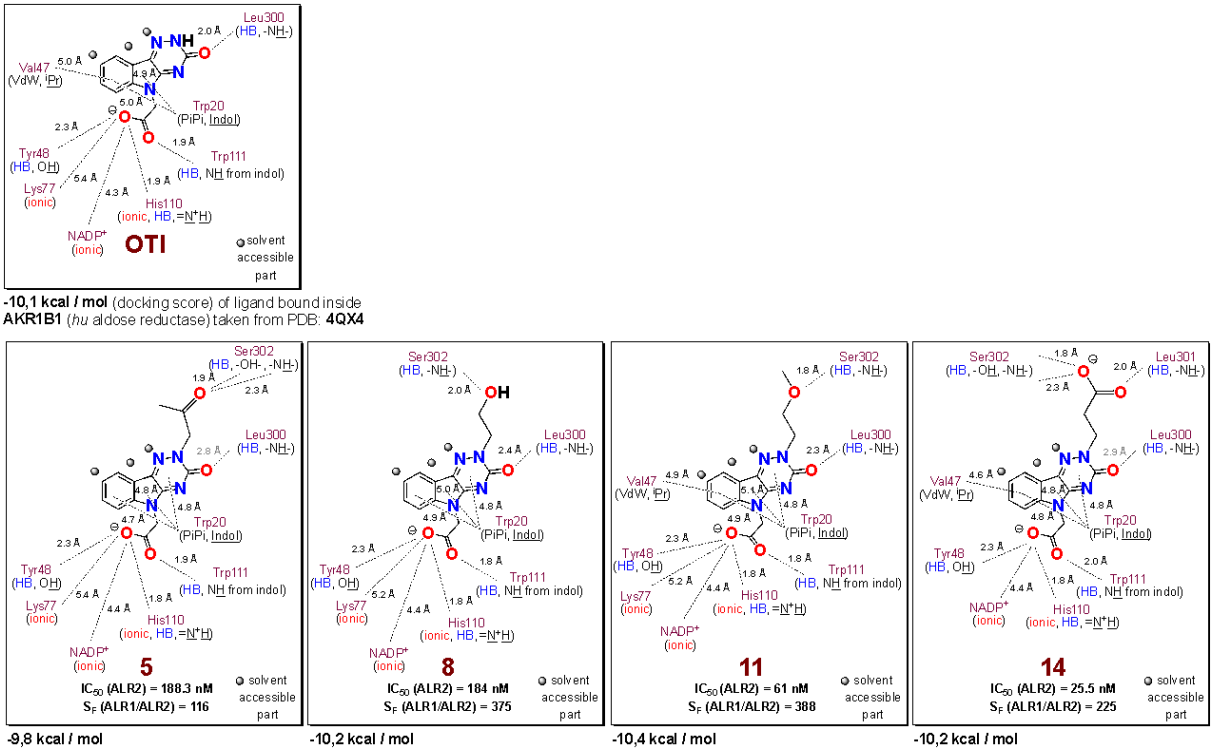

Figure 41. Interaction diagrams of OTI and its derivatives **5**, **8**, **11** and **14** obtained after analysis of docked ligands bound in an active site of AKR1B1 enzyme (from PDB: 4QX4).

4. Preparation of rat ALR2

ALR2 enzyme from rat lens was partially purified according to Hayman and Kinoshita (1965) as follows: lenses were quickly removed from rats following euthanasia and homogenized in a glass homogenizer with a teflon pestle in 5 volumes of cold distilled water. The homogenate was centrifuged at 10 000 g at 0-4 °C for 20 min. The supernatant was precipitated with solution of ammonium sulfate at 40 %, 50 % and then at 75 % of salt saturation. The supernatant was retained after the first two precipitations. The pellet from the last step, possessing ALR2 activity, was dispersed in 75% ammonium sulfate solution and stored in smaller aliquots in liquid nitrogen container.

5. Preparation of rat ALR1

ALR1 from rat kidney was partially purified according to the reported procedure of Costantino et al. (1999) as follows: kidneys were quickly removed from rats following euthanasia and homogenized in a knife homogenizer followed by processing in a glass homogenizer with a teflon pestle in 3 volumes of 10 mM sodium phosphate buffer, pH 7.2, containing 0.25 M sucrose, 2.0 mM EDTA dipotassium salt and 2.5 mM 2-mercaptoethanol. The homogenate was centrifuged at 16 000 g at 0-4 °C for 30 min and the supernatant was subjected to ammonium sulfate fractional precipitation at 40 %, 50 % and 75 % salt saturation. The pellet obtained from the last step, possessing ALR1 activity, was redissolved in 10 mM sodium phosphate buffer, pH 7.2, containing 2.0 mM EDTA dipotassium salt and 2.0 mM 2-mercaptoethanol to achieve total protein concentration of approximately 20 mg/mL. DEAE DE 52 resin was added to the solution (33 mg/mL) and after gentle mixing for 15 min removed by centrifugation. The supernatant containing ALR1 was then stored in smaller aliquots in liquid

nitrogen. No appreciable contamination by ALR2 in ALR1 preparations was detected since no activity in terms of NADPH consumption was observed in the presence of glucose substrate up to 150 mM.

6. *Enzyme assays*

NADPH, *D,L*-glyceraldehyde, sodium *D*-glucuronate were obtained from Sigma-Aldrich (St. Louis, MO, USA). Other chemicals were purchased from local commercial sources and were of analytical grade quality. Aldose reductase and aldehyde reductase activities were assayed spectrophotometrically by determining NADPH (0.12 mM final concentration) consumption at 340 nm and were expressed as decrease of the optical density (O.D.)/s/mg protein (Stefek et al. 2008). The effect of the tested compounds on enzyme activities was determined by their required concentrations in water. At the same concentration, the inhibitor was included in the reference blank. The reference blank contained all the above reagents except the substrate to make correction for oxidation of NADPH not associated with reduction of the substrate. The enzyme reaction was initiated by addition of a substrate (*D,L*-glyceraldehyde 5 mM final concentration) for ALR2 or sodium *D*-glucuronate for ALR1 (20 mM final concentration) and was monitored for up to 4 min after an initial period of 1 min at 30 or 37 °C, respectively. Enzyme activities were adjusted by diluting the enzyme solutions with distilled water so that 0.05 mL of the preparation gave an average reaction rate for the control sample of 0.020 ± 0.005 absorbance units/min. IC_{50} values were determined both from the least square analysis of the linear portion of the semilogarithmic inhibition curves and non-linear regression analysis. Each curve was generated using at least four concentrations of inhibitor causing an inhibition in the range from at least 25–75% in minimally triplicate repetitions.

References

A.V. Marenich, R.M. Olson, C.P. Kelly, C.J. Cramer, D.G. Truhlar, Self-Consistent Reaction Field Model for Aqueous and Nonaqueous Solutions Based on Accurate Polarized Partial Charges, J. Chem. Theory Comput. 3 (2007), 2011−2033. https://doi.org/10.1021/ct7001418.

E. Krieger, G. Vriend, YASARA View-Molecular Graphics for All Devices-From Smartphones to Workstations. Bioinformatics 30 (2014), 2981−2982. https://doi.org/ 10.1093/bioinformatics/btu426.

E. Krieger, J.E. Nielsen, C.A.E.M. Spronk, G.Vriend, Fast Empirical pKa Prediction by Ewald Summation, J. Mol. Graphics Modell. 25 (2006), 481−486. https://doi.org/ 10.1016/j.jmgm.2006.02.009.

J.A. Maier, C. Martinez, K. Kasavajhala, L.Wickstrom, K.E. Hauser, C. Simmerling, Ff14SB: Improving the Accuracy of Protein Side Chain and Backbone Parameters from ff99SB, J. Chem. Theory Comput. 11 (2015), 3696−3713. https://doi.org/10.1021/acs.jctc.5b00255.

L. Costantino, G. Rastelli, M.C. Gamberini, J.A. Vinson, P. Bose, A. Iannone, M. Staffieri, L. Antolini, A. Del Corso, U. Mura, A. Albasini, 1-Benzopyran-4-one antioxidants as aldose reductase inhibitors, J Med Chem. 42 (1999), 1881-1893.

L. Kovacikova, M. S. Prnova, M. Majekova, A. Bohac, C. Karasu, M. Stefek, Development of Novel Indole‑Based Bifunctional Aldose Reductase Inhibitors/Antioxidants as Promising Drugs for the Treatment of Diabetic Complications. Molecules 26 (2021), 2867. https://doi.org/10.3390/molecules26102867

M. Hlaváč, L. Kováčiková, M.Š. Prnová, P. Šramel, G. Addová, M. Májeková, G. Hanquet, A. Boháč, M. Štefek, Development of Novel Oxotriazinoindole Inhibitors of Aldose Reductase: Isosteric Sulfur/Oxygen Replacement in the Thioxotriazinoindole Cemtirestat Markedly Improved Inhibition Selectivity, J. Med. Chem. 63 (2020), 369-381. https://doi.org/10.1021/acs.jmedchem.9b01747.

M. Hlaváč M, L. Kováčiková L, M.Š. Prnová, G. Addová, G. Hanquet, M. Štefek, et al. Novel Substituted N-Benzyl(Oxotriazinoindole) Inhibitors of Aldose Reductase Exploiting ALR2 Unoccupied Interactive Pocket. Bioorg Med Chem. 29 (2020), 115885. https://doi.org/10.1016/j.bmc.2020.115885.

M. Majekova, J. Ballekova, M. Prnova, M. Stefek, Structure Optimization of Tetrahydropyridoindole-Based Aldose Reductase Inhibitors Improved their Efficacy and Selectivity, Bioorg. Med. Chem. 25 (2017), 6353−6360. https://doi.org/ 10.1016/j.bmc.2017.10.005.

M. Stefek, M. Soltesova Prnova, M. Majekova, C. Rechlin, A. Heine, G. Klebe, Identification of Novel Aldose Reductase Inhibitors Based on Carboxymethylated Mercaptotriazinoindole Scaffold, J. Med. Chem. 58 (2015), 2649-2657. https://doi.org/10.1021/jm5015814.

M. Stefek, V. Snirc, P.O. Djoubissie, M. Majekova, V. Demopoulos, L. Rackova, Z. Bezakova, C. Karasu, V. Carbone, O. El-Kabbani, Carboxymethylated pyridoindole antioxidants as aldose reductase inhibitors: synthesis, activity, partitioning, and molecular modeling, Bioorg Med Chem. 16 (2008), 4908-4920. https://doi.org/10.1016/j.bmc.2008.03.039.

S. Hayman, J. Kinoshita, Isolation and properties of lens aldose reductase, J Biol Chem. 240 (1965), 877-882.